Modeling bronchial circulation with application to soluble gas exchange: description and sensitivity analysis

THIEN D. BUI, 1 DONALD DABDUB, 2 AND STEVEN C. GEORGE1

Departments of ¹Chemical and Biochemical Engineering and Materials Science and of ²Mechanical and Aerospace Engineering, University of California, Irvine, California 92697-2575

Bui, Thien D., Donald Dabdub, and Steven C. George. Modeling bronchial circulation with application to soluble gas exchange: description and sensitivity analysis. J. Appl. Physiol. 84(6): 2070-2088, 1998.—The steady-state exchange of inert gases across an in situ canine trachea has recently been shown to be limited equally by diffusion and perfusion over a wide range (0.01-350) of blood solubilities (β_{blood} ; $ml \cdot ml^{-1} \cdot atm^{-1}$). Hence, we hypothesize that the exchange of ethanol ($\beta_{blood} = 1,756$ at 37°C) in the airways depends on the blood flow rate from the bronchial circulation. To test this hypothesis, the dynamics of the bronchial circulation were incorporated into an existing model that describes the simultaneous exchange of heat, water, and a soluble gas in the airways. A detailed sensitivity analysis of key model parameters was performed by using the method of Latin hypercube sampling. The model accurately predicted a previously reported experimental exhalation profile of ethanol ($R^2 = 0.991$) as well as the end-exhalation airstream temperature (34.6°C). The model predicts that 27, 29, and 44% of exhaled ethanol in a single exhalation are derived from the tissues of the mucosa and submucosa, the bronchial circulation, and the tissue exterior to the submucosa (which would include the pulmonary circulation), respectively. Although the concentration of ethanol in the bronchial capillary decreased during inspiration, the three key model outputs (end-exhaled ethanol concentration, the slope of phase III, and end-exhaled temperature) were all statistically insensitive (P > 0.05) to the parameters describing the bronchial circulation. In contrast, the model outputs were all sensitive (P < 0.05) to the thickness of tissue separating the core body conditions from the bronchial smooth muscle. We conclude that both the bronchial circulation and the pulmonary circulation impact soluble gas exchange when the entire conducting airway tree is considered.

mathematical model; Latin hypercube sampling; ethanol; pulmonary circulation; airways

GAS EXCHANGE EFFICIENCY is extremely dependent on the blood solubility (β_{blood} ; ml gas·ml blood⁻¹·atm⁻¹) of the gas. The major effort in respiratory physiology over the past four decades has been to characterize the exchange of gases with low (β_{blood} <0.1) -to-intermediate $(0.1 < \beta_{blood} < 100)$ blood solubility. This effort stemmed from the intermediate solubilities of the respiratory gases (β_{blood} for $O_2 = 0.7$ and β_{blood} for $CO_2 = 3$). However, the lungs exchange a wide variety of gases that range from low solubility, such as sulfurhexafluoride or helium ($\beta_{blood}=0.01$), to high solubility, such as water vapor ($\beta_{blood}=20{,}000$). The exchange of low- and intermediate-solubility gases occurs predominantly in the alveolar regions, with the airways providing a conduit for movement of gas between the alveoli and the ambient air. In contrast, the exchange of highly soluble gases ($\beta_{blood} > 100$) occurs primarily within the conducting airways (1, 6, 30, 31).

The absorption-desorption dynamics of a soluble gas are difficult to evaluate because of the relative inaccessibility of the airways to direct experimental measurement. A two-dimensional model of the airways previously developed in this laboratory and by others (12, 37) describes the simultaneous exchange of heat, water, and a highly soluble gas with the pulmonary airways and represents an avenue to understanding the exchange process. The soluble gas used in the model simulations is ethyl alcohol because of its high water and blood solubility ($\beta_{blood} = 1,756$) and because of its important applications in the medicolegal arena. The performance of the model has been compared with axial profiles of air temperature available in the literature (37) as well as exhalation ethanol profiles from human subjects (12). In these simulations, the bronchial capillary bed was assumed to be an infinite source/sink for ethanol and heat (i.e., no perfusion dependence). Most recently, experimental and theoretical data suggest that the exchange of gases spanning a wide range of solubilities (0.01 < β_{blood} < 350) demonstrates a similar perfusion dependence to exchange in the trachea (14, 35). These results indicate that our previous assumptions related to the bronchial circulation (infinite sink/ source) may not be valid.

In addition, the present model structure lumps the lamina propria and bronchial epithelium into a single nonperfused layer and does not include the bronchial smooth muscle as a distinct anatomic layer. Both the epithelium and the smooth muscle are important anatomic features of the airways that play critical roles in basic physiology (i.e., mucus secretion, immune response, airway caliber) and in airway pathology (i.e., bronchial asthma). Although the epithelium and the smooth muscle may not be critical to understanding the exchange of inert gases such as ethanol, they will be important in future airway gas-exchange simulations involving endogenous gases such as nitric oxide or pollutant gases such as ozone. Thus the objective of this study is threefold: 1) to design a more realistic description of the bronchial circulation for incorporation into the existing mathematical model; 2) to expand the radial description of the airway wall to include an epithelial layer, a smooth muscle layer, and a sink/ source that represents the core body; and 3) to perform a detailed sensitivity analysis of the model parameters to determine their relative importance in understanding soluble gas exchange in the airway.

EXPERIMENTAL METHODS

The experimental methods and data have been previously described and reported (12). As the focus and goals of this

manuscript are modeling airway gas exchange, only a summary will be presented here. Six male volunteers without previous history of cardiac or pulmonary disease and with normal physical examination findings served as subjects. Each subject ingested enough alcohol in the form of liquor to achieve a blood alcohol concentration of ~ 0.09 g/100 ml. After ingestion of alcohol, the subjects waited \sim 1 h for absorption to take place, which was monitored by sequential breath tests.

Ethanol concentration in the exhaled breath was measured with a commercially available infrared absorption breathtesting instrument (Intoxilyzer 5000). After passing through the Intoxilyzer 5000, the exhaled breath entered a wedge spirometer where exhaled volume and flow rate were measured. Each subject performed a series of single-exhalation or vital capacity maneuvers where exhalation flow rate was controlled. In a single-inhalation maneuver, the subject inhales to total lung capacity then exhales the vital capacity at a slow constant flow rate to residual volume. The breathing maneuver was repeated five times, each spaced by ~3 min of quiet nasal tidal breathing. Blood samples were taken from the antecubital vein at three points in time after the estimated start of the postabsorptive phase. Blood alcohol concentration was subsequently measured with a gas chromatograph (Perkin Elmer model 3920) by using headspace analysis (21).

For the purposes of this paper, a single representative exhalation profile from a human subject was of interest to test the overall performance of the model before the sensitivity analysis. Thus the exhalation profiles from the six subjects (30 profiles together) were condensed into a single profile as follows. First, a simple smoothing routine (average of 10 nearest neighbors) was performed on each exhaled profile. Next, the expired partial pressure of ethanol (P_E) was normalized by the concentration of ethanol in the alveolar gas (PA) $(P_A = C_{blood}/\beta_{blood})$, where C_{blood} is the measured venous blood concentration of ethanol). Thus the normalized concentration of ethanol in the air (\overline{P}_E) is plotted as function of exhaled volume (V). The five exhaled profiles for each subject were then truncated to the smallest exhaled volume of the group and consolidated into a single profile by taking the mean \overline{P}_E at one-tenth exhaled volume intervals. Finally, the consolidated profiles from each subject were combined by averaging the \overline{P}_{E} across all subjects. As each subject had a different exhaled volume, the final representative profile (see Fig. 3) has error bars associated with each axis.

ANALYTICAL METHODS

Glossary

- Surface area for exchange between the connective $A_{\rm c}$ tissue or the smooth muscle and the capillaries (cm^2)
- Surface area of cylinder of diameter d and length $A_{\rm d}$ Δz (cm²)
- Surface area between capillaries and smooth $A_{c,s}$ muscle tissue in length Δz (cm²)
- Surface area between capillaries and connective $A_{\rm c.t}$ tissue in length Δz (cm²)
- Solubility of gas in blood (ml gas⋅ml blood⁻¹⋅atm⁻¹) β_{blood} Solubility of gas in body-tissue layer (ml gas·ml blood $^{-1}$ ·atm $^{-1}$) β_{b}
 - Solubility of gas in epithelium (ml gas⋅ml blood⁻¹⋅ β_e atm^{-1}
 - Solubility of gas in air (1 ml gas · ml blood⁻¹ · atm⁻¹ β_g at 1 atm pressure)
 - β_{ij} Partial rank correlation coefficient

- Solubility of gas in mucous layer (ml gas ml $\beta_{\rm m}$ $blood^{-1} \cdot atm^{-1}$
- Solubility of gas in smooth muscle layer (ml gas · ml β_s blood $^{-1} \cdot atm^{-1}$)
- β_t Solubility of gas in connective tissue layer (ml $gas \cdot ml \ blood^{-1} \cdot atm^{-1})$
- C Molar concentration of tissue (assumed to have the properties of water) (mol/cm³)
- Concentration of ethanol in circulating blood (ml C_{blood} ethanol/ml blood)
 - C_{e} Molar density of ethanol (mass density divided by molecular weight) (mol/cm3)
 - Molar heat capacity of dry air ($J \cdot mol^{-1} \cdot K^{-1}$)
 - Molar heat capacity of ethanol vapor $(J \cdot mol^{-1} \cdot K^{-1})$
 - Molar heat capacity of liquid ethanol $(J \cdot mol^{-1} \cdot K^{-1})$
 - Molar heat capacity of liquid water $(J \cdot mol^{-1} \cdot K^{-1})$
- Molar heat capacity of water vapor $(J \cdot mol^{-1} \cdot K^{-1})$
- $\begin{array}{l} \hat{C}_{p,w}^g \hat{C}_{p,da}^g \left(\boldsymbol{J} \cdot \boldsymbol{mol}^{-1} \cdot \boldsymbol{K}^{-1} \right) \\ \hat{C}_{p,e}^g \hat{C}_{p,da}^g \left(\boldsymbol{J} \cdot \boldsymbol{mol}^{-1} \cdot \boldsymbol{K}^{-1} \right) \\ \text{Diameter of the airway (cm)} \end{array}$
- - Scaling factor in the range 1.1-2.5, which inδ creases the surface area of the airway lumen due to invaginations
- $D_{\rm e,a}$ Diffusivity of ethanol in air (cm²/s)
- $D_{\rm e,w}$ Diffusivity of ethanol in water (cm²/s)
- Diffusivity of ethanol in lung tissue (cm²/s) $D_{\mathrm{e,t}}$
- Ratio of the surface area of the capillaries to that $\xi_{c,t}$ of a cylinder with the same radius in the connective tissue
- Ratio of the surface area of the capillaries to that $\xi_{c,s}$ of a cylinder with the same radius in the smooth muscle
- Ratio between the volume of the capillaries and $\phi_{c,t}$ the total volume of tissue
- Ratio between the volume of the capillaries and $\phi_{c,s}$ the total volume of smooth muscle
- F Weighting factor for bronchial blood flow in connec-
- FScaling factor to maintain a constant ratio of conducting airway space to vital capacity
- Airway generation number g
- Scaling factor that allows the thickness of the body layer for energy transfer $(\gamma * I_b)$ to be larger than that of mass transfer (I_b)
- $\Delta H_{\rm v,e}$ Latent heat of evaporation for ethanol (J/mol)
- Latent heat of evaporation for water (J/mol) $\Delta H_{\rm v.w}$
- Local heat transfer coefficient between the lumen $h_{m,a}$ wall and the air $(J \cdot s^{-1} \cdot K^{-1} \cdot m^{-2})$
- Overall heat transfer coefficient between the body $h_{b,b}$ layer and the body $(J \cdot s^{-1} \cdot K^{-1} \cdot m^{-2})$
- $h_{b,s}$ Overall heat transfer coefficient between the body layer and the smooth muscle $(J \cdot s^{-1} \cdot K^{-1} \cdot m^{-2})$
- Overall heat transfer coefficient between the epi $h_{e.m}$ thelium and mucus $(J \cdot s^{-1} \cdot K^{-1} \cdot m^{-2})$
- Overall heat transfer coefficient between the per $h_{s,t}$ fusive tissue and smooth muscle $(J \cdot s^{-1})$ $K^{-1} \cdot m^{-2}$
- Overall heat transfer coefficient between the per $h_{t,e}$ fusive tissue and epithelium layer $(J \cdot s^{-1})$ $K^{-1} \cdot m^{-2}$
- Molar flux of ethanol from the mucous surface in .*j*e control volume (mol·s $^{-1}$ ·cm $^{-2}$)
- Total molar flux of fluid into the control volume .*J*fluid $(\text{mol}\cdot\text{s}^{-1}\cdot\text{cm}^{-2})$
- Total molar flux of ethanol from the body core J_{body}

 $P_{\text{E},\text{max}}$

(atm)

2072	MODELING THE BRONCHIAL			
	during both inspiration and expiration (mol/breath)	$\overline{P}_{E,ma}$		
$J_{ m br}$	Total molar flux of ethanol from the bronchial circulation during both inspiration and expiration (mol/breath)	P P P,		
$J_{ m e,exp}$	Total molar flux of ethanol from the mucous surface in an airway generation during expiration	P P		
$J_{ m e,insp}$	(mol/breath) Total molar flux of ethanol from the mucous surface in an airway generation during expiration	P_{c}		
$J_{ m h,exp}$	(mol/breath)Total molar flux of heat from the mucous surface in an airway generation during expiration (J/	P_c		
$J_{ m h,insp}$	breath) Total molar flux of heat from the mucous surface in an airway generation during inspiration (J/	$\dot{ ext{q}}_{ ext{br,}}$		
$J_{ m tiss}$	breath) Total molar flux of ethanol from the bronchial mucosa and submucosal tissue layers during	$\dot{ ext{q}}_{ ext{br}}$		
$J_{ m w,exp}$	both inspiration and expiration of single exhalation (mol/breath) Total molar flux of water from the mucous surface	$egin{aligned} \mathbf{Q}_{\mathrm{br}}, \ \dot{\mathbf{Q}}_{\mathrm{br}} \end{aligned}$		
$J_{ m w,insp}$	in an airway generation during expiration (mol/ breath) Total molar flux of water from the mucous surface in an airway generation during inspiration (mol/	<i>1</i> I		
$k_{ m m,a}^{ m e}$	breath) Local mass transfer coefficient of ethanol from the lung walls to the airway (mol·s ⁻¹ ·m ⁻² ·mole-	ρ _ι \$ Τ		
$k_{ m m,a}^{ m w}$	fraction ⁻¹) Local mass transfer coefficient of water from the lung wall to the airway (mol·s ⁻¹ ·m ⁻² ·mole-	${ m T}$ ${ m T}_{ m bod}$		
$k_{ m b,b}$	fraction ⁻¹) Overall mass transfer coefficient between the body and the body layer (cm/s)	- 500 Т Т		
$k_{ m b,s}$	Overall mass transfer coefficient between the smooth muscle and the body layer (cm/s) Overall mass transfer coefficient between the epi-	\mathbf{T}_1		
$k_{ m e,m}$ $k_{ m s,t}$	thelium layer and the mucous layer (cm/s) Overall mass transfer coefficient between the	$rac{T_{ m E,ma}}{T_{ m E,ma}}$		
$k_{ m t,e}$	smooth muscle and the tissue layer (cm/s) Overall mass transfer coefficient between the epithelium layer and the tissue layer (cm/s)	T, T		
$egin{array}{c} \kappa_{ m w} \ I_{ m b} \ I_{ m m} \end{array}$	Thermal conductivity of water $(J \cdot m^{-1} \cdot K^{-1} \cdot s^{-1})$ Thickness of body layer (cm) Thickness of the mucous layer (cm)	Т		
$egin{array}{c} I_{ m e} \ I_{ m t} \ I_{ m s} \end{array}$	Thickness of epithelium (cm) Thickness of connective tissue layer (cm) Thickness of smooth muscle (cm)	T_{c}		
$\begin{matrix} \lambda_{c,t} \\ \lambda_{s,t} \end{matrix}$	Capillary-tissue partition coefficient Smooth muscle-tissue partition coefficient	т с т		
$\lambda_{e,m}$ $\lambda_{m,a}$	Partition coefficient of ethanol between the epithe- lium layer and the mucous layer Partition coefficient of ethanol between mucus and air	T V		
$M_{ m w} \over n$	Molecular weight of water (g/mol) Compartment number	V _e		
n _c Ņ N	Number of capillaries Molar density of air (mol/l) Molar flow rate of air (mol/s)	V_c		
$egin{array}{c} \mathbf{P_{amb}} \\ \mathbf{P_{a}} \\ \mathbf{P_{E}} \end{array}$	Ambient pressure (atm) Arterial partial pressure of ethanol (atm) Expired partial pressure of ethanol (atm)	V_{c}		
P _{E,max}	Maximum expired partial pressure of ethanol (atm)	$V_{\rm T}$		

CHIAL CIR	CULATION
$\overline{P}_{E,\text{max}}$	Normalized (by arterial partial pressure) maximum expired partial pressure of ethanol
P_l	Airway luminal partial pressure of ethanol (atm)
$\mathbf{P_e}$	Partial pressure of ethanol in the epithelium (atm)
$P_{\rm m}$	Partial pressure of ethanol in the mucus (atm)
P_s	Partial pressure of ethanol in the smooth muscle (atm)
P_{t}	Partial pressure of ethanol in the connective tissue (atm)
$P_{c,s}$	Partial pressure of ethanol in the capillary (venous) of the smooth muscle (atm)
$P_{c,t}$	Partial pressure of ethanol in the capillary (venous) of the connective tissue (atm)
ģ	Normalized blood flow (ml·ml tissue ⁻¹ ·s ⁻¹)
$\mathbf{q}_{\mathrm{br,s}}$	Bronchial blood flow to a control element of the smooth muscle (ml/s)
$\dot{\mathbf{q}}_{\mathrm{br,t}}$	Bronchial blood flow to a control element of connective tissue (ml/s)
\mathbf{Q}_{br}	Total bronchial blood flow (1 ml/s)
$Q_{\mathrm{br,s}}$	Total bronchial blood flow to the smooth muscle (0.5 ml/s)
$ m \dot{Q}_{br,t}$	Total bronchial blood flow to the connective tissue (0.5 ml/s)
r	Radius of the airway (cm)
$r_{\rm c}$	Average radius of a capillary (cm)
R	Ideal gas constant (8.314 $J \cdot K^{-1} \cdot mol^{-1}$)
ρ _w Ś	Density of water (g/ml) Secretion rate of fluid from the epithelium to
T_1	mucus (mol·s ⁻¹ ·cm ⁻²) Temperature of air in the control volume of the
	lumen (K)
$egin{array}{c} T_{ m b} \ T_{ m body} \end{array}$	Average temperature of the body layer (K) Temperature of the core body and arterial blood (K)
$rac{\mathrm{T_c}}{\mathrm{T_e}}$	Temperature of blood in the capillary (K) Average temperature of the epithelium in the con-
т	trol volume (K)
${ m T_E}$	Expired temperature (K) Maximum (or end-expired) temperature (K)
$\frac{T_{E,max}}{T_{E,max}}$	Normalized (by body temperature) maximum (or end-expired) temperature
$T_{\rm m}$	Average temperature of mucus in the control vol- ume (K)
T_s	Average temperature of the smooth muscle layer (K)
T_{t}	Average temperature of the connective tissue layer (K)
$T_{c,s}$	Temperature of the smooth muscle capillary blood (K)
$T_{c,t}$	Temperature of the connective tissue capillary blood (K)
$\tau_{\rm s}$	Residence time of blood in the smooth muscle capillary (s)
$ au_{t}$	Residence time of blood in the connective tissue capillary (s)
V	Expired volume (ml)
V_{ee}	Lung volume at end-expiration (ml)
V _{ei}	Lung volume at end-inspiration (ml)
$egin{array}{c} V \ V_{\mathrm{c,t}} \end{array}$	Volumetric flow rate of the airstream (ml/s) Volume that capillaries occupy in the control ele-
$V_{c,s} \\$	ment of the connective tissue (ml) Volume that capillaries occupy in the control ele-
$V_{\rm m}$	ment of the smooth muscle (ml) Volume of control element of mucus (liters)
$V_{\mathrm{T,t}}^{\mathrm{m}}$	Total volume of the control element of connective tissue control element (ml)
	` '

 $V_t \qquad \text{Volume that tissue mass occupies in the control} \\ \text{element (ml)}$

 X_a Average mole fraction of ethanol in arterial blood (equal to X_{body})

 X_b Average mole fraction of ethanol in the bodytissue layer

 $\begin{array}{c} X_{body} & \text{ Average mole fraction of ethanol in the core body} \\ & \text{ (equal to } X_a) \end{array}$

 $X_{c,t}$ Average mole fraction of ethanol in the connective tissue capillary

 $X_{c,s}$ Average mole fraction of ethanol in the smooth muscle capillary

X_m Average mole fraction of ethanol in mucus

X_e Average mole fraction of ethanol in epithelium

X_s Average mole fraction of ethanol in the smooth muscle layer

X_t Average mole fraction of ethanol in the connective tissue layer

Y_e Mole fraction of ethanol in air

 $Y_{e,wall}$ Mole fraction of ethanol at the mucus-air interface

Y_w Mole fraction of water in the air

 $Y_{w,wall}$ Mole fraction of water at the mucus-air interface Length of control element (cm)

Lung Model

The mathematical model is described in detail elsewhere (13, 37). The important new features, including a detailed description of the new bronchial circulation and additional radial layers, are described in detail here; the final governing equations are derived, in brief, and summarized in the APPENDIX. The model describes the simultaneous exchange of heat, water, and an inert gas with the airways. The initial detailed description and sensitivity analysis were described by Tsu et al. (37). Since then, the model has had several modifications, each one adding a new level of sophistication as our understanding of airway gas exchange has improved.

Axial structure. The axial structure of the model is unchanged and consists of a symmetrical bifurcating structure through eighteen Weibel generations. The respiratory bronchioles and alveoli are currently lumped together into a single respiratory unit that is justified for heat and highly soluble gas exchange. The dimensions (lengths and diameters) of the airways for the upper respiratory tract (nasal and oral) are taken from Hanna (15) and those for the lower respiratory tract are from Weibel (39). Because the volume of the conducting airways increases with increasing lung volume, the dimensions of the lower airways are scaled by using the parameter F such that the ratio of the volume of the conducting airways to the vital capacity is maintained constant. The vital capacity of the lungs used by Weibel was \sim 5,075 ml; hence, F is defined as

$$F = \left(\frac{\text{VC}}{5,075}\right)^{1/3} \tag{1}$$

where VC is the vital capacity of the lungs being simulated. The lengths and diameters from Weibel's data are then multiplied by F thus maintaining a constant ratio of length to diameter as well as a constant ratio of conducting airway volume (propor-

tional to length \times diameter²) to vital capacity. The upper and lower respiratory tract and airways are divided into 480 axial control volumes, as depicted in Fig. 1, A and B.

Radial structure. GENERAL. The previous radial structure of the airway control volume is depicted in Fig. 1 A and consisted of four compartments: 1) the airway lumen; 2) a thin layer of mucus; 3) a nonperfused tissue layer that represents the respiratory epithelium, basement membrane, and any connective tissue before reaching 4) the capillary bed of the bronchial circulation. The capillary bed was considered an infinite source or sink for heat and the soluble gas; that is, the temperature and concentration of the soluble gas in the bronchial circulation were fixed.

In the new model (Fig. 1B), the airways are now divided into seven radial compartments: 1) the airway lumen, 2) a thin mucous layer, 3) the epithelium, 4) a connective tissue layer (i.e., the lamina propria) perfused by the bronchial circulation, 5) the bronchial smooth muscle layer perfused by the bronchial circulation, 6) a body-tissue layer that acts as a buffer to heat and mass transport between the core body conditions and the smooth muscle layer, and 7) the core-body layer.

Over the majority of the airway tree, the radius of the airway lumen is much larger than the thickness of the radial layers; thus the surface area for exchange between the radial compartments within each control volume is practically constant and approximately equal to $2\pi r\Delta z$, where r is the radius of the airway lumen and Δz is the axial length of the control volume (with the notable exception of the mucus-air interface, see below). All radial tissue or liquid-phase layers are considered a dilute binary mixture of water and a soluble gas (ethanol). Axial diffusion is neglected, except in the gas phase. Radial transport between the layers occurs by molecular diffusion (Fick's first law) and secretion and/or filtration (see below and APPENDIX for specific details in each layer). The inert-gas concentration and temperature gradients within each radial layer are considered linear between the midpoint and the interface of the adjacent compartment(s) (see APPENDIX).

AIRWAY LUMEN. The air is considered a system of dry air, water vapor, and a single inert gas. The small exchange of respiratory gases with the airways is considered negligible. At ambient pressure and over the range of temperatures expected within the lung, air behaves as an ideal gas. Longitudinal or axial diffusive transport is included in the gas phase. An effective axial diffusion coefficient ($D_{\rm e,a,eff}$) is used, which reflects the experimental observations of Scherer et al. (29) that account for enhanced axial diffusion due to secondardy convective flows induced by the bifurcations

$$D_{\rm e,a,eff} = D_{\rm e,a} (1 + 1.08 N_{\rm Pe}),$$
 inspiration (2)

$$D_{\rm e.a.eff} = D_{\rm e.a} (1 + 0.37 N_{\rm Pe}),$$
 expiration (3)

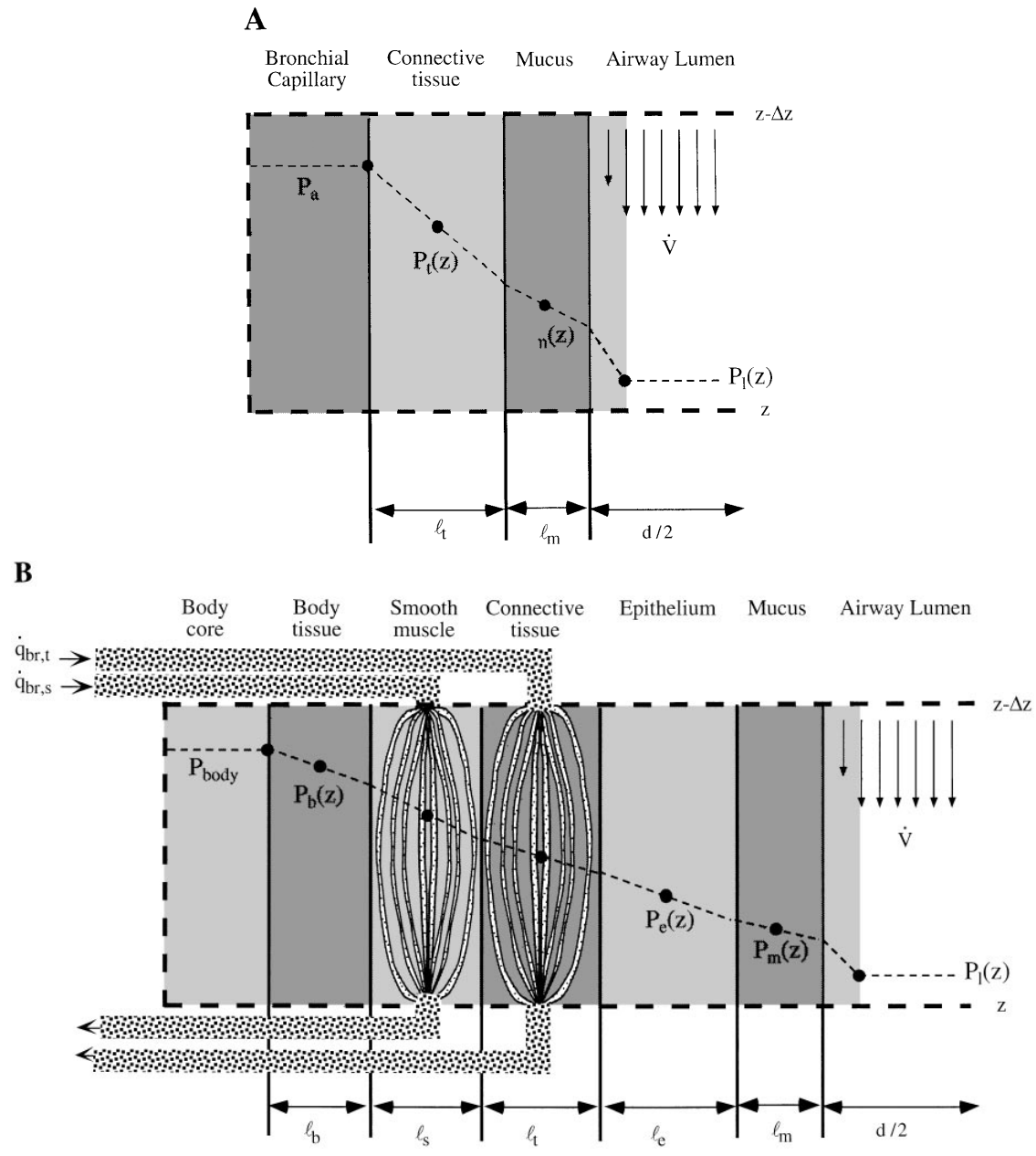


Fig. 1. Model control volume. A: previous model that includes only 4 radial layers and assumes that bronchial capillary bed is an infinite source or sink for heat and ethanol. B: new model that now includes 7 radial layers and a dynamic description of bronchial circulation to both lamina propria and smooth muscle, and a body compartment that represents an infinite sink or source of ethanol and heat. Blood enters capillary compartments with a partial pressure (P_a), ethanol then diffuses across a series of radial resistance before entering the passing airstream. Approximate linear partial pressure profiles in each radial compartment are depicted. Mass transfer by diffusion between radial layers is described by product of an overall transfer coefficient and the partial pressure difference between compartments at midpoints. Shaded region in airway lumen represents aerodynamic resistance due to mucus-air interface. See Glossary for symbol definitions.

where $N_{\rm Pe}$ is the Peclet number $[ud/D_{\rm e,a}]$, where u is the mean axial velocity of the airstream (cm/s), d is the airway diameter, and $D_{\rm e,a}$ is the molecular diffusion coefficient of ethanol in air at 37°C (0.128 cm²/s)]. Transport between the mucous layer and gas phase is described with heat and mass transfer coefficients. The heat transfer coefficient (h), is taken from an empirical correlation derived by Ingenito (18), and the correspond-

ing mass transfer coefficient is calculated from the Chilton-Colburn analogy (5).

During the inspiratory and expiratory phases of respiration, the lung expands and contracts to draw and expel air from the alveoli. This results in a slight stretching and compressing of the airway walls. In addition, during bronchoconstriction there is conservation of the airway lumen perimeter. As a result, the

luminal surface of the airway wall contains luminal folds or currugations (19). It is unclear from the report of Weibel (39) whether luminal folds were considered in the measurement of airway diameters and, hence, in the calculation of luminal surface area. Thus, δ is a scaling parameter that accounts for enhanced surface area due to mucosal folds such that $\delta = 1$ when there are no mucosal folds. To attain a rough estimate of δ , we empirically examined cross-sectional histological images of the airways (9) by measuring the perimeter of the airways with and without consideration of the mucosal folds. It was observed that the degree to which the wall is corrugated increases as the generation number increases until approximately the 12th generation. The value of δ was found to be \sim 2.5 in the small airways; δ was found to be 1.1 at the trachea and was scaled linearly to the 12th generation to a value of 2.5. The δ value was then held constant at 2.5 for the remainder of the airway tree. It should also be noted that incorporating δ into the surface-area calculation improved the model's ability to simulate the phase III slope (S_{III} ; see RESULTS, Single exhalation). Derivation of the energy and mass balance within the airway lumen as well as the remaining layers can be found in APPENDIX.

MUCUS. Because mucus is $\sim\!95\%$ water, the physical properties of the mucous layer (subscript m) are equivalent to these of water. A variable mucous layer thickness is incorporated into the model to account for local hydration and dehydration. Fluid is secreted into the mucous layer from the epithelium if the thickness of the mucus falls below a minimum value. The minimum value ($I_{\rm m}$) is 10 $\mu {\rm m}$ in the trachea (25) and is scaled to smaller values in the lower generations such that the volume of mucus in each generation is equivalent to that in the trachea. This assumption is based on the observations that the mucous layer is thinner in smaller airways (32) and that the volume of mucus in each generation is constantly swept caudally toward larger airways, including the trachea.

BRONCHIAL EPITHELIUM. The physical properties of the epithelium (subscript e) are assumed to be equal to these of water, with the exception of solubility and diffusivity. Because blood and tissue have similar water and lipid contents, the tissue is assumed to have the solubility properties of blood. The diffusion coefficient of ethanol in the respiratory mucosa has been experimentally determined to be 5.63×10^{-6} cm²/s, which is approximately one-third of the diffusion coefficient of ethanol in water (11). The epithelium secretes fluid to the mucous layer to maintain a minimum thickness of the mucous. In order for the epithelium to maintain a constant volume (or thickness), an equimolar volume of fluid enters the epithelium from the adjacent perfused connective tissue layer. The thickness of the epithelium $(I_{\rm e})$, is determined from data of Gastineau et al. (10) (100 μ m in the trachea, 20 μ m in the bronchioles).

PERFUSED CONNECTIVE TISSUE AND SMOOTH MUSCLE. All physical properties of the connective tissue (subscript t) and smooth muscle (subscript s) are assumed to be equal to those of water, with the exception of solubility

and diffusivity, as described above for the epithelium. Fluid is secreted from the nonperfused tissue layer to the epithelium, as described above, and replaced by filtration from the bronchial circulation within the connective tissue layer. No fluid is secreted from the smooth muscle layer because of its anatomical distance from the mucous layer relative to the perfused connective tissue.

The blood flow to the connective tissue and smooth muscle layers is modeled as an evenly dispersed network of capillaries that supplies blood at the condition of the body and exits at a new condition, which is determined by the dynamics of heat and mass transfer. The bronchial blood flow to the smooth muscle layer $(Q_{br.s})$ is assumed to be equal to that of the connective tissue (Q_{br,t}) on a unit volume of tissue basis, such that the the sum of the two circulations for the entire airway tree (\hat{Q}_{br}) is equal to 1 ml/s [~1% of the cardiac output (23)]. It has been previously demonstrated that \sim 90% of the blood flow to the smooth muscle originates from the bronchial circulation (38). The average radius of the capillary (r_c) is set equal to 10 μ m (22), and the mean residence time (τ) of the blood in the control volume is set to 1 s (40). The number of capillaries (n_c) necessary to achieve the above stipulations is then calculated as simply the ratio of the total volume of the capillary bed and the volume of one capillary

$$n_{\rm c} = \frac{\dot{\mathbf{q}}_{\rm br} \tau}{\pi r_{\rm c}^2(\Delta z)} \tag{4}$$

where \dot{q}_{br} is the bronchial blood flow to each control volume. Once the number of capillaries is known, the surface area for exchange between the connective tissue or the smooth muscle and the capillaries (A_c) is simply $n_c(2\pi r_c \Delta z)$. If Eq.~2 is substituted into the definition of A_c , then the bronchial circulation in each layer (smooth muscle or connective tissue) can be described by four parameters $(A_c,~\tau,~r_c,~and~\dot{q}_{br})$ by the following relationship

$$A_{\rm c} = \frac{2\dot{\mathbf{q}}_{\rm br}\tau}{r_{\rm c}} \tag{5}$$

Hence, if any three parameters are chosen, the fourth is fixed. In our analysis, A_c is calculated by Eq. 5, and the three remaining parameters are incorporated into the sensitivity analysis (Table 1).

Blood entering the connective tissue and smooth muscle layers has a partial pressure of gas that is equal to P_a and body temperature (T_{body} , 37°C). Blood within the capillaries is considered well mixed (no axial gradient within each control volume); it exchanges heat and mass with the tissue compartment and exits with a partial pressure P_c (equivalent to venous) and temperature of blood in the capillary (T_c).

The axial distribution of blood flow to the smooth muscle is uniform; that is, each control volume has the identical blood flow on a unit volume of tissue basis (0.0407 ml blood·ml tissue $^{-1} \cdot s^{-1}$). The axial distribution of the remaining bronchial circulation to the

Table 1. Model parameters, uncertainty range, and central values

Symbol	Model Parameter	Uncertainty, %	Central Value	Ref. No.
$r_{\rm c}$	Average radius of capillary	±20	10 μm	22
$ar{\dot{\mathbf{q}}}_{\mathrm{br,s}}$	Normalized blood flow rate to smooth muscle	± 50	$0.0407~\mathrm{ml}\cdot\mathrm{s}^{-1}\cdot\mathrm{ml}~\mathrm{muscle}^{-1}$	23
$ar{\dot{\mathbf{q}}}_{\mathrm{br,t}}$	Normalized blood flow rate to tissue	± 50	$0.0407~\text{ml}\cdot\text{s}^{-1}\cdot\text{ml}~\text{tissue}^{-1}$	23
h	Local heat transfer coefficient from air to mucus	± 50	Calculated	18
k	Local mass transfer coefficient from air to mucus	± 50	Calculated	5
$I_{ m m}$	Minimum thickness of mucous layer	± 20	10 μm in trachea	25
$I_{ m e}$	Thickness of epithelial layer	± 10	100-20 μm (trachea -18th gen)	10
I_{t}	Thickness of tissue layer	± 20	$30\%~l_{ m e}$	26
$l_{\rm s}$	Thickness of smooth muscle	± 20	5–14% of $I_{\rm e}$ (upper-low airway)	26
$I_{\rm b}$	Thickness of body layer for mass transport	± 80	$14 imes l_{ m e}$	
γ	Scaling factor to determine thickness of body layer for heat transport	± 80	9	
κ_{t}	Thermal conductivity of tissue	± 10	$0.633~{ m J}\cdot{ m s}^{-1}\cdot{ m m}^{-1}\cdot{ m K}^{-1}$	28
$D_{ m e,t}$	Diffusivity of ethanol in tissue	± 10	$5.63 imes10^{-6}$ cm 2 /s	11
$D_{ m e,a,eff}$	Effective diffusivity of ethanol in air	± 10	Insp: $D_{e,a}$ (1 + 1.08 N _{pe}) Exp: $D_{e,a}$ (1 + 0.37 N _{pe})	29
$\lambda_{e,m}$	Epithelium-mucus partition coefficient	± 20	0.823	21
$\lambda_{m,a}$	Mucus-air partition coefficient	± 20	2,134 at 37°C	21
τ_{t}	Residence time in tissue layer capillaries	± 20	1 s	40
τ_{s}	Residence time in smooth muscle capillaries	± 20	1 s	40
F	Size factor which scales lengths and diameters of airways, based on the subjects' vital capacity	± 20	1.0	39
δ	Scaling factor that accounts for increased surface area of the lumen due to corrugations	± 20	1.1–2.5 (trachea to 12th gen)	_

Insp, inspiration; Exp, expiration; gen, generation.

connective tissue layer is described by an exponential dependence on axial position recently described by Bernard et al. (2). The blood flow rate to control volume \boldsymbol{x} is defined by the following relationship

$$\dot{\mathbf{q}}_{\mathrm{br},t}(\mathbf{x}) = \mathbf{V}_{\mathrm{T},t}(\mathbf{x})\dot{\bar{\mathbf{q}}}_{\mathrm{br},t}\mathbf{F}(\mathbf{x}) \tag{6}$$

where $V_{T,t}(x)$ is the total volume of tissue in the control volume (cm³), F(x) is a weighting factor given by Bernard et al. (2), and $\dot{\bar{q}}_{br,t}$ is the mean control volume blood flow on a unit volume of tissue basis (0.0407 ml blood·ml tissue⁻¹·s⁻¹). These parameters are defined

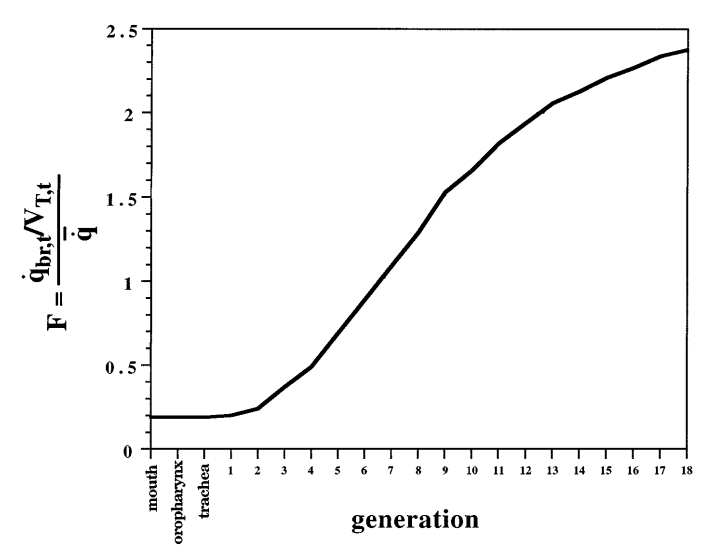


Fig. 2. Blood flow to connective tissue normalized by tissue volume is inversely related to airway diameter, based on work by Bernard et al. (2). F represents tissue-volume-normalized blood flow to each compartment normalized by mean value of tissue-volume-normalized flow for entire airway tree. See *Glossary* for symbol definitions.

by the following relationships

$$V_{T,t}(x) = \pi dl_t(x) \Delta z \tag{7}$$

$$F(x) = 0.19 + (2.8)e^{-0.51d(x)}$$
 (8)

$$\bar{\dot{\mathbf{q}}}_{\mathrm{br,t}} = \frac{\dot{\mathbf{Q}}_{\mathrm{br,t}}}{\sum_{\mathbf{x}} \mathbf{V}_{\mathrm{T,t}}(\mathbf{x})} \tag{9}$$

where d(x) is the airway diameter (mm). Figure 2 plots F as a function of airway generation. Note that the blood flow per unit volume of tissue in the upper airways is approximately an order of magnitude smaller than in the bronchioles and that the mean normalized blood flow $(\bar{q}_{br,t})$ occurs at approximately *generation 7* (F 1). Details of the energy and mass balances within the connective tissue and smooth muscle leading to the governing equations can be found in APPENDIX.

BODY-TISSUE. A layer of "body-tissue" (subscript b) was added into the model as a buffer between the main body compartment and the radial compartments. The body-tissue does not represent a distinct anatomical layer that is present in vivo; rather, the extra layer is a necessary model construct, since the radial distance from the smooth muscle at which the conditions of the body (i.e., 37°C and P_a) exist is unknown. The thickness of the body layer, I_b , represents the distance from the smooth muscle interface, where the partial pressure of ethanol and the temperature are constant at Pa and T_{body}, respectively. Because thermal diffusivity is approximately two orders of magnitude larger than the mass diffusivity of ethanol, the effective thickness of the body layer will be larger for heat transfer. This effect is accounted for by a scaling factor (γ) , such that the thickness of the body layer for heat transfer is $I_b \gamma$.

CORE BODY. The core body layer represents an infinite sink or source of heat and mass in the model. The partial pressure of ethanol and the temperature are considered constant at P_a and 37° C, respectively.

Boundary conditions. To calculate concentrations of the species at the airway wall, local vapor-liquid equilibrium is assumed at the air-mucus interface. Raoult's law is applied to water, and β_w is used for the soluble gas. The ratio of solubilities between blood and connective tissue (β_{blood}/β_t) and between blood and smooth muscle (β_{blood}/β_s) is set equal to unity, and between the epithelium and mucus (β_e/β_m) is set equal to the β_{blood}/β_w ratio. At the interface between each of the compartments, it is assumed that there is no net accumulation of energy or mass such that flux of energy and mass between adjacent compartments is continuous. During inspiration, the concentration of the soluble gas in the ambient air is considered to be zero. The temperature and water content of the inspired air are user-controlled variables but are held constant during a simulation. During expiration, the air that leaves the alveoli has the following properties: 1) it is fully saturated with water, 2) its temperature is equal to body temperature, and 3) the partial pressure of the soluble gas is in equilibrium with the blood as described by β_{blood} .

Computer Simulation

The mass and energy balances produce 16 dependent variables and 2 independent variables (time and position). The APPENDIX summarizes the sixteen coupled partial differential equations. The system of partial differential equations is solved numerically by using a UNIX-based computer. The spatial derivatives are handled with upstream finite differencing, whereas the time derivatives are solved using LSODE, a time-integration software package developed by Hindmarsh (17).

Before simulating a single exhalation maneuver, the model must simulate 30 tidal breaths to reach steadystate conditions for temperature and concentration profiles in the airway lumen, mucus, and tissue regions (36). A respiratory rate of 12 breaths/min, a sinusoidal flow waveform, and a tidal volume approximated as 10% of the subject's vital capacity (16) were used. For all simulations, inspired air temperature was 23°C and relative humidity 50%. Inspired volume, expired volume, inhalation time, and exhalation time must be specified to simulate a single exhalation maneuver. Inspired volume was determined based on the assumption that each subject inhaled to total lung capacity; inspired volume can then be approximated as 65% (16) of the subject's mean vital capacity (0.65 \times 5,400 ml = 3,510 ml). Expired volume was equal to the mean minimum value for all six subjects (4,160 ml), as described in the EXPERIMENTAL METHODS and RESULTS. Inhalation time was equal to that during tidal breathing (2.5 s), and inhalation flow rate was assumed constant at a value equal to inspired volume divided by inspiration time. The exhalation time (20.8 s) for each

condensed single-exhalation maneuver can be determined by dividing the expired volume by the mean flow rate (200 ml/s) of the experimental exhalation maneuvers.

Sensitivity Analysis

The method of Latin hypercube sampling (LHS) (27), was chosen to perform the sensitivity and uncertainty analysis. The advantage of using LHS rather than Monte Carlo for sensitivity analysis is that it substantially reduces the number of simulations needed for an adequate analysis of numerical or computer models (27). LHS has been used successfully in the field of atmospheric chemistry to analyze the sensitivity and uncertainty in complex atmospheric models (7).

Table 1 summarizes the characteristics (central values and uncertainty ranges) of 20 parameters in the model judged to have the greatest uncertainty or impact on the model output. Broadly, the 20 parameters include those that describe the bronchial circulation and physical features of the airways, such as solubility, diffusivity, surface area, and diffusing distance. The choice of uncertainty ranges is subjective and based on the method used to obtain the central value. For example, since there is no information on the parameters $l_{\rm b}$ and γ , they were assigned a high level of uncertainty ($\pm 80\%$), whereas the diffusivity of ethanol in air, $D_{\rm e,a}$, and ethanol in tissue, $D_{\rm e,t}$, which were based on careful experimental measurements, were assigned an uncertainty range of only $\pm 10\%$.

To perform the LHS analysis, the model simulates the exhalation profile two times the number of free or uncertain parameters. Thus, for 20 parameters, the model simulates the exhalation profile under 40 different conditions or sets of parameter values. The values for each parameter during each of the 40 simulations are chosen by using the following algorithm. Each variable is assigned a series of random numbers between 1 and 40 without replacement (each number is used only once). The random number is then converted into a multiplying factor (a factor that multiplies the central value), which is based on the uncertainty range defined for the variable (see Table 1). For example, if a random number of 1 appears under a variable that has an uncertainty of 20% for a specific run, then the multiplying factor for the variable used in that run would be 0.80. During each run, the choice for the specific multiplier of the central value is chosen completely randomly but without replacement.

The last step in the sensitivity analysis is to determine a quantitative sensitivity index for each of the 20 parameters and establish a threshold to identify those parameters to which the model output is sensitive and those to which the model output is insensitive. In LHS, the sensitivity index for each parameter is the respective partial-rank correlation coefficient, $\beta_{i,j}$, as defined by the following relationship

$$Y_i^k = \alpha + \beta_{i,1} X_1^k + \beta_{i,2} X_2^k + \dots + \beta_{i,20} X_{20}^k$$
 (10)

where Y is the value of the model output variable, α is a constant, X is the value for the model input variables, the superscript k refers to the simulation number (i.e., 1–40), and the subscript *i* refers to the specific model output. Linear least squares regression is implemented to determine the values for $\beta_{i,b}$, then a simple statistical test (t-statistic) is employed to determine whether each $\beta_{i,j}$ is statistically different (P < 0.05) from zero. If $\beta_{i,j}$ is different from zero, then we can conclude that it has a significant impact on model output i. Three model outputs were chosen that best reflect heat and mass transfer dynamics and that can also be easily measured experimentally: 1) normalized (by body temperature) end-exhaled airstream temperature ($\overline{T}_{E,max}$); 2) normalized (by alveolar partial pressure) end-exhaled airstream partial pressure of ethanol (\overline{P}_{Emax}); and 3) the normalized (by the maximum value of $S_{\rm III}$ for the 40 simulations) $S_{\rm III}$ of the exhalation ethanol profile ($S_{\rm III}$). All three model outputs were normalized such that the maximum value is one. $S_{\rm III}$ (liters⁻¹) is calculated from a linear least squares fit of the model output over the last one-half of the exhaled volume.

Several of the parameters in the model are calculated based on other parameters. For example, the thickness of the connective tissue layer is calculated as a fraction of the thickness of the epithelium layer. To obtain a sensitivity coefficient that is representative of only that parameter, each parameter is changed independently of the others. For example, the tissue thickness is calculated from the base value of the epithelium thickness and is not dependent on how the epithelium thickness is varied for the 40 simulations.

Airway Ethanol Flux

As a subject inhales, the airstream has the potential to absorb ethanol from the airways, more specifically, from the mucous layer that lines the airways. Over the course of an entire inspiration, each airway generation will contribute to the overall flux of ethanol from the mucus to the air. Over the course of an expiration, a portion of the ethanol absorbed on inspiration is desorbed back to the airways. The total flux of ethanol (mol/breath) from airway compartment n during either inspiration, $J_{e,insp}(n)$, or expiration, $J_{e,exp}(n)$, is simply the number of airway branches in the generation multiplied by the sum of the flux from each individual control volume

$$J_{e,insp}(n) = 2^{g} * \left[\frac{\delta(n) A_d(n)}{\dot{V}_{insp}(n)} \right] * \sum_{x+1}^{i} \left[\int_{V_{ee}}^{V_{ei}} j_e(x, V) \, dV \right] \quad (11)$$

$$J_{\text{e,exp}}(n) = 2^{g} * \left[\frac{\delta(n) A_{d}(n)}{\dot{V}_{\text{evn}}(n)} \right] * \sum_{x=1}^{i} \left[\int_{\text{Vei}}^{\text{Vee}} j_{\text{e}}(x, \text{V}) \, d\text{V} \right] \quad (12)$$

where $j_{\rm e}$ is the flux of ethanol from the mucous surface in each control volume as defined by the local mass transfer coefficient (see APPENDIX, Eq.~A3); \dot{V} is the volumetric flow rate of air (cm³/s) during inspiration and expiration, respectively; $V_{\rm ee}$ is the lung volume at

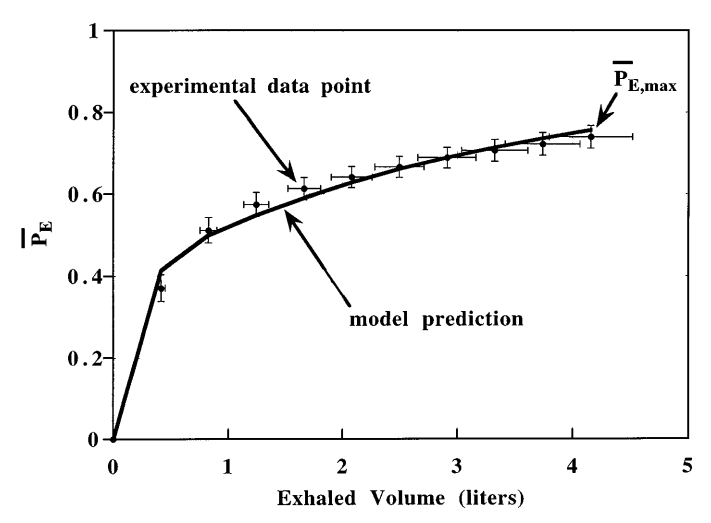


Fig. 3. Experimental and model-predicted exhaled ethanol profiles for a representative human subject. Experimental data are given by (\bullet). Model fit to data (solid line) was optimized by using thickness of body-tissue layer, I_b , as no experimental estimate of this parameter exists. This method is validated by sensitivity analysis. \overline{P}_E , normalized expired partial pressure of ethanol; $\overline{P}_{E,max}$, normalized maximal expired partial pressure of ethanol.

end expiration, V_{ei} is the lung volume at end inspiration, and g is the generation number. The differential time element $\mathrm{d}t$ has been transformed to a differential volume by $\mathrm{d}V = \dot{V}\,\mathrm{d}t$. Similar expressions can be easily derived to define the total molar flux of water $(J_{\mathrm{w,insp}})$ and $J_{\mathrm{w,exp}}$ and $J_{\mathrm{h,exp}}$ from each airway generation during a breath, as well the flux of ethanol between other compartments, most notably, the flux of ethanol from the bronchial capillaries (J_{br}) and the flux of ethanol from the body core (J_{body}) .

RESULTS

Experimental Single-Exhalation Maneuver

Detailed results of the experimental protocol have been previously published (12); hence, only the salient results will be presented here. The mean age, weight, vital capacity, and minimum exhaled volume for the single-exhalation maneuver for the six subjects were 30 ± 10 (SD) yr, 78 ± 14 kg, $5{,}400 \pm 740$ ml, and $4,160 \pm 810$ ml, respectively. The range for the mean exhaled flow rates for the six subjects was 140-320 ml/s, and the mean exhaled flow rate for all six subjects was 200 ± 70 ml/s. The average exhalation profile (as described in EXPERIMENTAL METHODS) is depicted in Fig. 3. Note that the concentration of ethanol in the exhaled breath increases immediately after the start of exhalation, demonstrating exchange in the airway space, and that phase III has a positive slope similar to that of other gases such as CO_2 and N_2 . The mechanism underlying the positive \mathcal{S}_{III} of ethanol differs from relatively insoluble gases such as CO₂ and N₂ and is related to a temporal heterogeneity in the partial pressure of ethanol in the airway tissue during exhalation. This mechanism is described in much greater detail in a previous paper (12).

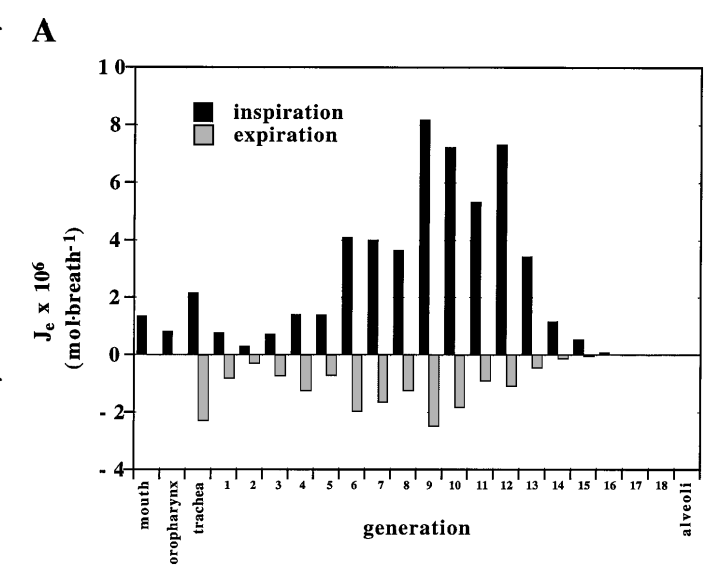
Model Simulation

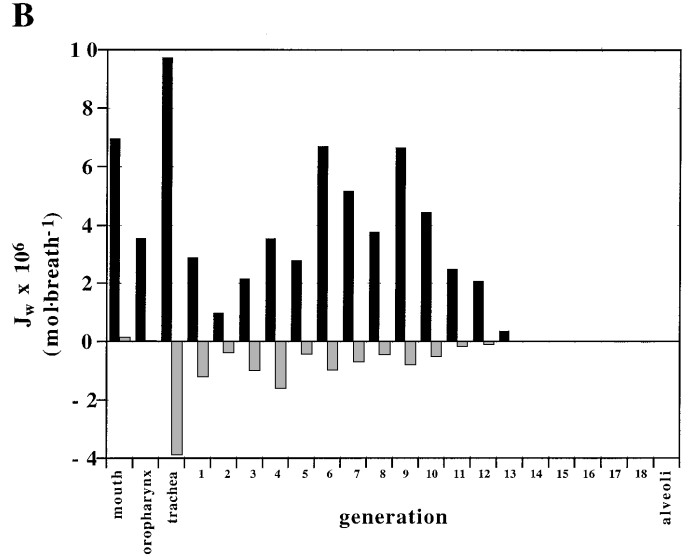
Single exhalation. Estimates for the central values of all model parameters were available (see Table 1) from data in the literature, except for the parameters associated with the thickness of the body layer (I_b and γ). Hence, I_b and γ were utilized to perform an initial optimization of the fit of the model prediction to the experimental exhaled ethanol profile and the endexhaled temperature, respectively, by minimizing the sum of squares of the error. Initially, the model prediction of the exhalation profile overestimated the initial concentration of ethanol in phase III and, hence, produced a smaller $S_{\rm III}$. This systematic error in the model could be overcome by enhancing the desorption of ethanol to airway wall in the smaller airways by incorporating the parameter δ in the calculation of the airway wall surface area $A_{\rm d}$, as described above. The optimal fit of the model is presented in Fig. 3. The model predicts well the shape of the single exhalation with a coefficient of determination (R^2) of 0.991. The optimal value for I_b was 14 times the thickness of the epithelium l_e . Then, in the trachea, where $l_e = 100 \, \mu m$, $I_{\rm b}=1.4$ mm, and in the bronchioles (generations 11-18), where $l_{\rm e}=20~\mu{\rm m},~l_{\rm b}=0.28~{\rm mm}.$ To simultaneously match the reported value of 34.6°C for the mean end-exhaled temperature of the breath (20), the optimal value for γ was 9; in other words, the thickness of the body layer for heat transfer (product $l_b \gamma$) is 126 times the value of the epithelium. In the trachea and bronchioles, this would correspond to \sim 1.26 and 0.25 cm, respectively.

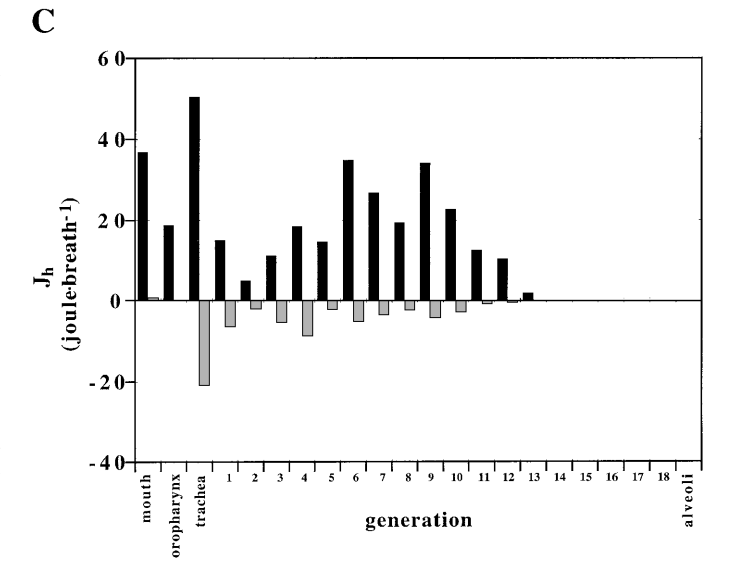
Axial flux distribution. Model predictions for the axial flux distribution from the mucus to the airstream for the single-exhalation maneuver (vital capacity of 5,400 ml, exhaled volume of 4,160 ml, and a flow rate of 200 ml/s) for ethanol, water, and heat are presented in Fig. 4, A-C, respectively. A positive flux denotes transfer of ethanol, water, or heat from the mucus to the airstream (absorption), a negative flux denotes flux from the airstream to the mucus (desorption).

The inspiratory and expiratory flux profiles for ethanol demonstrate a bimodal distribution with peaks in the trachea and 12th generation. $J_{\rm e,insp}$ becomes progressively smaller after the 9th generation and is nearly zero in 17th generation. Thus the model predicts that the incoming airstream reaches a local equilibrium with the capillary blood before reaching the alveoli; thus the exchange of ethanol in the lungs occurs entirely within the conducting airway space. During expiration, a portion (33%) of the ethanol absorbed by the airstream during inspiration is desorbed. The rate of desorption during exhalation decreases, thus account-

Fig. 4. Axial flux (J) distribution for ethanol during inspiration and expiration for ethanol (A; $J_{\rm e}$), water (B; $J_{\rm w}$), and heat (C; $J_{\rm h}$). Note bimodal distribution in A-C and that all 3 components reach a local equilibrium with body conditions before reaching alveolar region. Hence, model predicts that the exchange of ethanol, water, and heat occurs entirely within airway space.







ing for the positive $S_{\rm III}$. The total amount of ethanol eliminated from the lungs during the single-exhalation maneuver is 36.1 µmol/breath. This pattern of absorption-desorption is similar to prior predictions made by the model (12).

The inspiratory and expiratory flux profiles for water and heat are similar to these of ethanol, with the notable exception that they predict a local equilibrium with the core body conditions proximal to those of ethanol. For water and heat, the peak flux occurs in the trachea and *generation 6*, and the flux is nearly zero by *generation 13*. Hence, the model predicts that inspired air is fully warmed and humidified by approximately the 13th generation.

Figure 5 plots the net (inspiration plus expiration) axial flux distribution of ethanol into the airstream subdivided into three potential sources: I) contribution from the bronchial circulation ($J_{\rm br}$), 2) contribution from the body core to the body tissue ($J_{\rm body}$), and 3) contribution from the mucosal and submucosal tissues ($J_{\rm tiss}$; i.e., mucus, epithelium, connective tissue, smooth muscle, and body tissue). $J_{\rm br}$ is bimodal, with peaks in the trachea and 10th generation. $J_{\rm body}$ does not have a significant contribution in the extrathoracic airways but, rather, a rapid rise beginning in the 5th generation to a peak in the 11th generation. The sum of the flux of ethanol from the bronchial circulation and from the body core for the entire airway tree is 10.3 and 16.0 μ mol/breath, respectively (29 and 44% of total ethanol

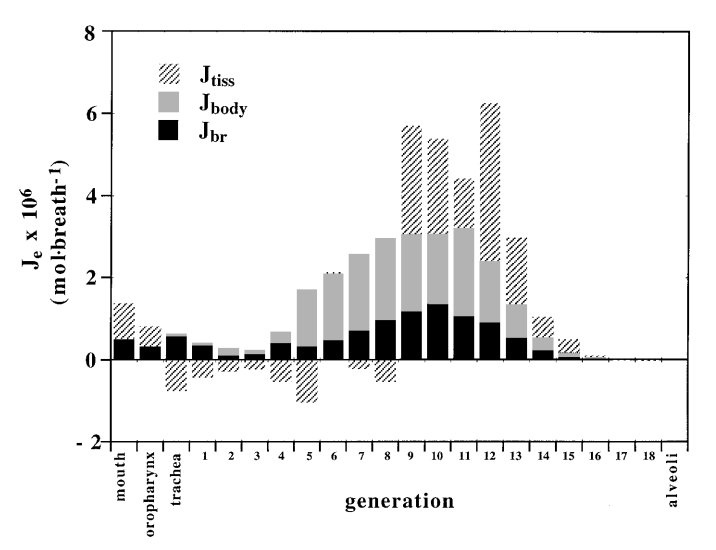


Fig. 5. Net axial flux distribution of ethanol into airstream during both inspiration and expiration. For each generation, net accumulation in airstream is a combination of contribution from body core $(J_{\rm body})$, bronchial circulation $(J_{\rm br})$, and surrounding mucosal and submucosal tissues $(J_{\rm tiss},$ mucus, epithelium, connective tissue, smooth muscle, and body layer). Hence, net accumulation presented here is equal to net flux presented in Fig. 4A from bronchial circulation $(J_{\rm br})$, the core body $(J_{\rm body})$, and the mucosal and submucosal tissues during single exhalation maneuver. Positive flux denotes flux from blood to the adjacent tissues or from body core to body tissue layer. In the case of $J_{\rm tiss}$, a positive value denotes a net increase in moles of ethanol present in mucosal and submucosal tissue (mol/breaths). Note that $J_{\rm body}$ is $\sim\!\!2$ -fold larger than $J_{\rm br}$ in the airway tree but is $\sim\!\!0$ in upper respiratory tract. This is consistent with the presence of pulmonary circulation surrounding intrathoracic airways.

eliminated). The remaining ethanol eliminated in the exhaled airstream (9.8 µmol/breath or 27%) of the transient single exhalation arises from the tissues of the mucosa and submucosa. $J_{\rm tiss}$ is positive in the mouth, oropharynx, and *generations* 9–16 but is negative in the trachea and *generations* 1–8. Although not shown, the flux is positive during both inspiration and expiration for both $J_{\rm br}$ and $J_{\rm body}$.

Figure 6 plots the axial distribution of the partial pressure of ethanol in the blood exiting the capillary bed (venous blood, $P_{c,t}$ and $P_{c,s}$) normalized by the incoming P_a at end inspiration and at end expiration for the single-exhalation maneuver. Both $P_{c,t}$ and $P_{c,s}$ fall below P_a during inspiration. This result indicates that the exchange process of ethanol is limited, at least in part, by the rate of blood flow from the bronchial circulation and is consistent with our hypothesis and with the results of recent investigations (14, 35). During expiration, the partial pressure of ethanol in the capillaries increases as ethanol is desorbed from airstream back to the airway wall (Fig. 4A) but does not entirely recover to P_a at end expiration.

Sensitivity analysis. The exhalation profiles (both ethanol concentration and temperature) for the 40 simulations in the LHS analysis are presented in Fig. 6. Figure 7A represents the range of exhalation ethanol profiles, and Fig. 7B represents the range for the exhalation temperature profile. The partial rank correlation coefficients (and their corresponding P values) from the LHS analysis are summarized in Table 2. Coefficients that have a P value <0.05 are bold-faced, whereas those with a P value >0.95 are italicized.

There is only one parameter, $l_{\rm b}$, to which all three of the model outputs are statistically sensitive. From this we conclude that the thickness of the effective buffer layer between the smooth muscle and the core body is one of the most significant parameters in predicting heat and mass exchange. We can use this result to either direct future experiments aimed at measuring this parameter more accurately, or, more likely, use this parameter to optimize the fit of the model and determine what a reasonable value may be. This is, in fact, what was done before the sensitivity analysis in an effort to gain an estimate of its central value.

There are three additional parameters to which both $P_{E,max}$ and the S_{III} are sensitive: $k_{m,a}^e$, $\lambda_{e,m}$, and $\lambda_{m,a}$ (P < 0.002 for both $P_{E,max}$, and S_{III}). These results are not surprising and serve to validate qualitatively the performance of the model. $P_{E,max}$ is also sensitive to I_t (P = 0.033), γ (P = 0.007), and δ (P = 0.004), whereas an additional parameter to which S_{III} is sensitive is F(P = 0.001). F is a parameter that scales the lengths and diameters of the airways to maintain a constant ratio of the volume of the conducting airways to the vital capacity. Two additional parameters to which exhaled temperature is sensitive are the local heat transfer coefficient between the mucous layer and the air ($h_{m,a}$) (P = 0.002) and γ (P = 0.001).

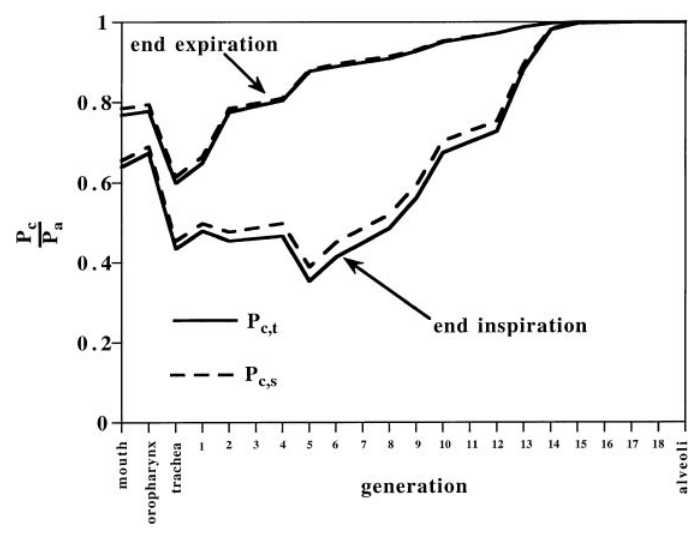


Fig. 6. Axial distribution of normalized (by arterial pressure) partial pressure of venous blood exiting capillary compartments of both tissue layer (lamina propria) and smooth muscle layer at end inspiration and end expiration. Note that partial pressure falls below that of the arterial blood during inspiration and does not completely recover during expiration. Hence, exchange of ethanol within airway space depends on blood flow rate of bronchial circulation. See *Glossary* for symbol definitions.

Parameters to which the model output is statistically insensitive (P > 0.95) also provide useful information. Each model output is insensitive to at least one parameter. $P_{E,max}$ is insensitive to the heat transfer coefficient (P = 0.97) and the thermal conductivity of the tissue

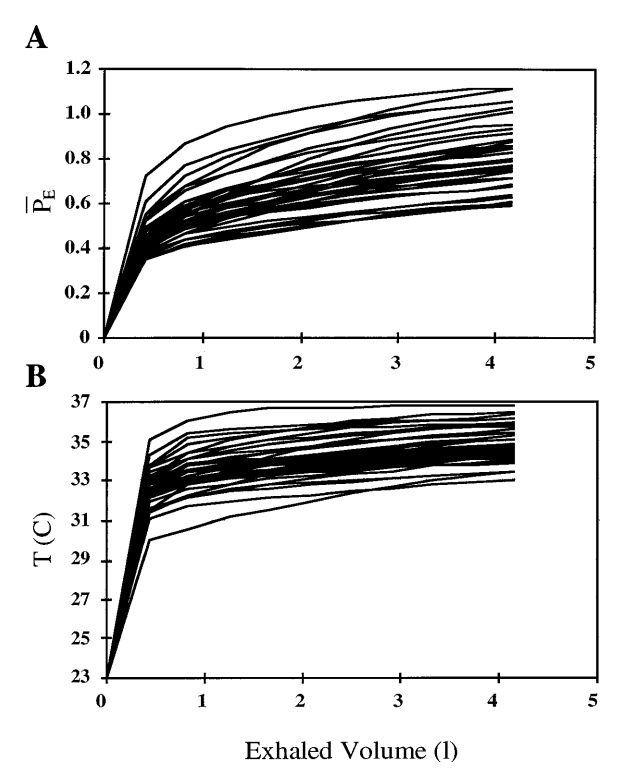


Fig. 7. Model ouput for the 40 simulations of Latin hypercube sampling. A: exhalation ethanol profile. B: exhalation temperature (T) profile.

Table 2. *Sensitivity coefficients* ($\beta_{i,i}$)

			Model O	utput		
	$\overline{\mathbf{P}}_{\mathrm{E,max}}$		$\overline{T}_{E,max}$		$\overline{S}_{ m III}$	
Variable	$\beta_{1,j}$	P	$\beta_{2,j}$	P	$\beta_{3,j}$	P
$r_{\rm c}$	0.075	0.054	0.0034	0.86	-0.027	0.83
$ {Q}_{br,s}$	0.031	0.090	-0.0017	0.86	0.013	0.82
$\dot{\mathbf{Q}}_{\mathrm{br,t}}$	0.020	0.15	0.0038	0.59	0.012	0.79
$h_{m,a}$	-0.0005	0.97	-0.028	0.002	0.022	0.66
$k_{ m m,a}^{ m e}$	-0.11	0.001	0.0090	0.25	0.17	0.002
$I_{\rm m}$	-0.016	0.66	-0.0088	0.65	0.0004	0.99
$I_{ m e}$	-0.14	0.062	-0.028	0.45	-0.13	0.58
I_{t}	-0.083	0.033	0.014	0.46	-0.098	0.42
$l_{\rm s}$	-0.014	0.71	-0.015	0.47	0.15	0.26
$I_{ m h}$	-0.094	0.001	-0.032	0.001	0.096	0.004
γ	-0.030	0.007	-0.029	0.001	0.040	0.24
κ_{t}	-0.0033	0.97	-0.075	0.093	0.36	0.19
$D_{ m e,t}$	0.14	0.14	-0.040	0.40	0.31	0.29
$D_{ m e,a,eff}$	-0.053	0.49	0.030	0.46	-0.043	0.86
$\lambda_{e,m}$	-0.71	0.001	0.011	0.61	-0.83	0.001
$\lambda_{m,a}$	-0.82	0.001	0.0064	0.75	-0.75	0.001
τ_{t}	-0.013	0.34	0.0021	0.76	-0.060	0.18
τ_{s}	-0.027	0.13	-0.011	0.23	0.065	0.26
F	0.040	0.27	0.038	0.053	-0.46	0.001
δ	-0.046	0.004	0.0001	0.99	-0.0082	0.86

 $\overline{S}_{\rm III}$, averaged slope of phase III; $D_{\rm e,a,eff}$, effective diffusivity of ethanol in air. Values in boldface, P < 0.05; values in italic, P > 0.95. For other symbols, see *Glossary*.

(P=0.97). This result is expected and can be used to qualitatively validate the performance of the model. $T_{\rm E,max}$ is insensitive to δ (P=0.99), whereas $S_{\rm III}$ is insensitive to the thickness of the mucous layer (P=0.99).

It is important to note that, although many of the parameters listed in Table 2 are not statistically significant, this does not mean that they are unimportant and have no impact on the model. What it does mean is that within their uncertainty range there was no particularly strong correlation between the input variable and the selected model output.

DISCUSSION

Blood Flow Rate and Perfusion Limitation

The decrease in partial pressure of ethanol in the blood during inspiration is due to the flux of ethanol from the blood through the tissue and mucous layers and into the passing airstream, creating the positive flux $J_{e,insp}$ seen in Fig. 4. The fact that $P_{c.t}$ and $P_{c.s}$ decrease during inspiration demonstrates a perfusion limitation to the exchange of ethanol in the airways. This contrasts with the earlier assumption made in the model, namely, that due to ethanol's large blood solubility, the delivery rate in the blood could be assumed to be infinite. The result is consistent with the experimental results of Souders et al. (35), who demonstrated a perfusion dependence to the exchange of acetone (β_{blood} 350) in the trachea. As blood solubility increases, the delivery rate (product $Q_{br}\beta_{blood}$) in the blood increases. However, the solubility in the tissue layer also increases; hence, the rate of diffusion of the gas through the tissue layer (which is proportional to solubility) increases a comparable amount. Thus, over a wide range of solubility, the relative dependence of gas exchange on perfusion and diffusion is independent of blood solubility (14). Of particular interest is the fact that the parameters associated with the bronchial circulation (blood flow rate, residence time, and capillary radius: $\dot{q}_{br,s}$, $\dot{q}_{br,t}$, τ_s , τ_t , and r_c , respectively) do not meet the statistical requirement of being sensitive. This is due to the close proximity of the pulmonary circulation, which represents an enormous source and sink for ethanol in our model (represented by the body layer) and in the experimental profiles. Note that in the experiments by Souders et al. (35) only exchange in the trachea was considered, which precludes the pulmonary circulation and accounts for sensitivity of the exiting tracheal gas concentrations to bronchial blood flow rate. This does not completely preclude these variables and, hence, the bronchial circulation, from influencing the exchange of ethanol, as demonstrated in Fig. 5. Note that their respective P values for $P_{E,max}$ (0.09, 0.15, 0.13, 0.34, and 0.054) are all <0.5 and are thus more likely to influence P_{E.max}. This is also consistent with the calculation demonstrating that 29% of exhaled ethanol in a single-exhalation maneuver is derived from the bronchial circulation. Although this is smaller than J_{body} (44%), which includes the pulmonary circulation, it is certainly not negligible.

Blood and/or Water Solubility

It has been previously established that the exchange dynamics of a gas within the lung are strongly dependent on the blood-to-gas $(\lambda_{b,a})$ or water-to-gas $(\lambda_{m,a})$ partition coefficient of the gas (4, 8, 31). The fact that $\lambda_{m,a}$ and $\lambda_{e,m}$ have a large impact on the exchange dynamics of ethanol comes as no surprise; in fact, this result represents a means of validating the performance of the model. Quite simply, as the solubility of a gas in blood or water is increased, the interaction with the airways increases because tissue is $\sim\!80\%$ water and mucus is $\sim\!95\%$ water (24). Thus the rate of desorption of a gas during exhalation is enhanced, resulting in a lower $P_{E,max}$ as well as a smaller S_{III} .

Diffusion Coefficient

The diffusion coefficient is an index of the relative ease with which a molecule can diffuse through a medium. The larger the diffusion coefficient, the easier it is for a molecule to diffuse and the lower the resistance. The diffusion of molecules in tissue has been studied extensively, and the consensus is that the diffusion coefficient in tissue of small (mol wt <100) molecules is $\sim\!30\text{--}40\%$ of their diffusion coefficient in water. Recently, the diffusion coefficient of ethanol in the respiratory mucosa was measured and found to be $5.63\times10^{-6}~\text{cm}^2/\text{s}$ or 34% of its value in water (11). The molecular diffusion of ethanol in tissue has been used

previously in this model as a free parameter to optimize the model's prediction of ethanol exchange, yet the present sensitivity analysis demonstrates that the key model outputs related to the exhalation profile ($P_{\rm E,max}$ and $S_{\rm III}$) are not statistically sensitive to $D_{\rm e,t}$. This is most likely due to the small uncertainty range ($\pm 10\%$) used in the model simulations due to the recently determined experimental value. Despite the small uncertainty range, the P values (0.14 and 0.29 for $P_{\rm E,max}$ and $S_{\rm III}$, respectively) demonstrate that $D_{\rm e,t}$ has a significant impact on the exchange dynamics of ethanol.

Thickness of Diffusion Barrier

The thickness of the tissue barriers in the model plays an important role, as the tissue barriers serve as diffusion barriers between the airstream and the source of ethanol or heat (i.e., the core body or the bronchial circulations). The thicknesses of the mucous and epithelial layers are not statistically significant, although the P value for $l_{\rm e}$ was 0.062 for $P_{\rm E,max}$. This result is explained, in part, by the fact that I_e is well characterized (10) (hence the small uncertainty of 10%) and that $I_{\rm m}$ is very small (maximum thickness of 10 μ m). The sensitivity of P_{E,max} to the thickness of the connective tissue can be explained by its relative proximity to the airway lumen (compared with the smooth muscle) and the fact that the connective tissue contains a source of ethanol. The fact that $T_{E,max}$ is insensitive to the thickness of all of the tissue layers (except l_h) is due to the relatively rapid diffusion of heat (two orders of magnitude larger) compared with the diffusion of mass.

The tremendous sensitivity of all model outputs on the thickness of the body-tissue layer indicates that the core body conditions are the greatest contributors to the exchange of ethanol and heat. In particular, the pulmonary circulation is in close proximity to the airways, beginning at approximately the 4th generation, and, due to its large volumetric flow rate (two orders of magnitude larger than the bronchial circulation), represents an enormous source of ethanol and heat. In addition, the pulmonary circulation has been previously shown experimentally to have a large impact on intra-airway heat exchange (33). Hence, the pulmonary circulation dictates the thickness of the body layer in the model and, thus, has a larger impact on ethanol exchange than does the bronchial circulation.

As I_b is not a true anatomic barrier but, rather, a model construct, it is difficult to comment on the absolute value attained by the model. However, the value of 1.68 mm for the transfer of ethanol in the trachea certainly seems reasonable. In addition, the value of 1.34 cm for heat transfer also seems reasonable based on the data of Solway et al. (34), who reported cooling of the esophageal lumen during cold air hyperpnea. One simplification that may be a source of error is the use of a single value for I_b and γ in the entire airway tree. The fact that the exchange of both

ethanol and heat is heterogeneous in the axial direction (see Fig. 4) indicates that the distance from the smooth muscle where the core body conditions exist (i.e., $\lambda_b \gamma$) is also heterogeneous. For example, the exchange of heat is essentially complete by the 12th generation; hence, I_b may be effectively zero (and not 0.39 cm) in the bronchioles and larger in the oropharynx and trachea, where the exchange of heat is substantial. The impact of introducing an axial dependence to I_b will be addressed in future simulations.

Local Mass Transfer Coefficient

The local mass transfer coefficient $k_{m,a}^e$ describes the transport of ethanol across the mucus-air interface. Values for the model are taken from Ingenito (18), who measured intrathoracic airway temperatures (from nasal cavity to the 6th generation) and then used a model of the airways to determine an average heat transfer coefficient for the entire airway tree from the trachea to the bronchioles. The correlation has the form Nu = 0.227*(Re*Pr)^{0.668}, where Nu is the Nusselt number (proportional to the heat transfer coefficient), Re is the Reynolds number (proportional to airstream velocity), and Pr is the Prandtl number. The corresponding mass transfer coefficient is calculated from the Chilton-Colburn analogy (5). Thus the model must extrapolate by using the Ingenito correlation to determine mass transfer coefficients for generations 7-18, as no experimental data exist for this region.

The correlation predicts that the mass transfer coefficient decreases monotonically as airstream velocity decreases. However, as airstream velocity decreases and flow transitions from turbulent to laminar (transition occurs at approximately Re <2,100), the heat and mass transfer coefficients reach an asymptote and become independent of further decreases in velocity (3, 14). Thus, in *generations 7–18*, where airflow is very slow (Re <5 during inspiration to total lung capacity in 2.5 s), it is very likely that the correlation predicts a mass transfer coefficient that is too small. In addition, the impact of the mass transfer coefficient on the resistance to airway gas exchange is substantial for a gas that has blood solubility as high as that of ethanol (14), as solubility in the gas phase is independent of solubility in water and tissue. These two concepts, combined with the exceptionally small P values for k(0.001 and 0.002 for $P_{E,max}$, and S_{III} , respectively) demonstrate the extreme importance of $k_{\rm m,a}^{\rm e}$ in accurately describing airway gas-exchange dynamics. The probable underestimation in $k_{\mathrm{m,a}}^{\mathrm{e}}$ might also explain the observed improved ability of the model to simulate the $S_{\rm III}$ when the surface area of the smaller airways is enhanced by δ . The flux of ethanol from the airway wall is proportional to the product $\emph{k}_{\mathrm{m,a}}^{\mathrm{e}}\emph{A}_{\mathrm{d}}$; hence, an improved simulation of the $S_{\rm III}$ could also have been attained with a larger value for $k_{\rm m,a}^{\rm e}$ in the smaller airways. Additional studies to more accurately describe

the factors that influence $k_{\mathrm{m,a}}^{\mathrm{e}}$ are planned for the future

Surface Area

The surface area of the airway lumen is considered in the sensitivity analysis by two variables, δ and F. The δ is the scaling factor in the airway lumen used to increase the surface area of the lumen to account for mucosal folds in the luminal surface, particularly in the smaller airways. Not surprisingly, P_{E,max} is quite sensitive to this parameter ($\bar{P} = 0.004$). An increase in the surface area enhances the recovery (or desorption) of ethanol at a constant rate during exhalation, resulting in a decrease in the concentration of ethanol in the exhaled breath. The effect of δ is independent of time, as δ scales the desorption flux of ethanol by the same magnitude at each point in time. Hence, the slope of the exhalation profile is unaffected. Interestingly, $T_{E,max}$ is insensitive to δ and can be explained by the fact that an increase in δ enhances the recovery of both heat and mass (as opposed to the heat transfer coefficient). The recovery of heat by the airways acts to cool the airstream; however, this effect is offset by the recovery of mass that is accompanied by the latent heat of vaporization (in this case condensation), which tends to warm the mucous layer. Tsu et al. (37) demonstrated that latent heat transfer comprises ~80-90% of the total respiratory heat exchange. Our estimate of δ as described in METHODS was crude, and it serves only as an initial attempt to investigate the possible importance of mucosal folds. The report of Weibel (39), which was used in determining airway diameter and, hence, airway surface area, does not explicitly state whether mucosal folds were present or accounted for in the measurement of airway diameter. In addition, as mentioned earlier, the same effect on the model prediction of the exhalation profile could be attained by enhancing $k_{\mathrm{m,a}}^{\mathrm{e}}$ in the smaller airways. The results of the sensitivity analysis suggest that more careful investigation into the magnitude of δ is justified.

F is a scaling factor that increases the size of the airway tree based on the subject's vital capacity, such that the volume of the airways is always the same percentage of the vital capacity. Both the lengths and the diameters of the airways are increased as the vital capacity is increased. Interestingly, an increase in F (which increases the total surface area of the airway lumen) does not have a statistical impact on P_{E,max} but it does have a very significant impact on $S_{
m III}$. This is the opposite response to δ . The difference can be attributed to the effect of increasing the volume (as F does) of the airways and not just the surface area (as δ does). Recall that by increasing F, the volume of the airways is increased by increasing both the length and diameter of the airway. A larger d corresponds to an increase in the Reynolds number (proportional to d) but a decrease in the linear velocity of the flow (inversely proportional to d²). Hence, the net result is a decrease in the Reynolds number, which results in a smaller mass transfer

coefficient (proportional to the $Re^{0.688}$). Hence, the larger surface area for recovery of ethanol is partially offset by a reduced efficiency of transfer across the gas-phase film resistance. The rate of ethanol recovery remains enhanced, such that the increase in F results in a smaller $S_{\rm III}$.

Conclusions

A model of the bronchial circulation has been incorporated into a larger model that simulates the simultaneous exchange of heat, water, and a soluble gas in the airways. The model was tested by using experimental exhalation ethanol profiles from human subjects. The model predicts that ethanol exchange occurs entirely within the airway tree but that the bronchial circulation is not necessarily the sole source of exhaled ethanol. The exchange dynamics of ethanol are particularly sensitive to three variables, which include the local mass transfer coefficient between the airstream and the airway wall, the solubility in blood and/or water, and the thickness of an effective layer of tissue separating or buffering the smooth muscle from the core body conditions. The thickness of this buffering layer is likely to depend strongly on the pulmonary circulation, which is in close proximity to the airways and serves as an enormous sink of both ethanol and heat. In addition, the flux of ethanol from the body core (which would contain the pulmonary circulation) accounts for 44% of the exhaled ethanol. Hence, we conclude that the exchange of ethanol depends on both the bronchial circulation and the pulmonary circulation.

The results of this study suggest a more prominent role of the pulmonary circulation in the exchange of highly soluble gases than previously thought when the arterial blood is the source of the gas. Additional experimental information, in particular on the heat and mass transfer coefficients in the lower airways, is needed for future simulations.

APPENDIX

Material and energy balances in each of the radial compartments are presented below. Although derivations of the material and energy balances with the airway lumen and mucous layer have been previously described in detail (13, 37), several minor changes have been made; thus, their derivation is presented again, in brief.

The governing equations are derived by performing energy and mass balances on each compartment. The volume of each radial compartment, except for the mucous layer, is assumed to be constant. The radial compartments are also assumed to have the same total molar concentration (C) as water and can be expressed as $C = \rho_w/M_w$, where ρ_w is the density of water, and M_w is the molecular weight of water. Concentrations in the radial compartments are written in terms of mole fractions. The mole fraction of ethanol (X) is related to the partial pressure P by $X = P\beta\,C_e/C$, where β is solubility in the medium (atm $^{-1}$), and C_e is the molar density of ethanol (mol/cm 3).

An overall transfer coefficient for heat or mass can be easily estimated from either Fourier's law of heat conduction or

Fick's first law of diffusion, respectively. By assuming a linear concentration or temperature profile, the flux of heat or mass can be written as the thermal or mass diffusivity divided by the length of diffusion and multiplied by the concentration or temperature difference across the length. The diffusivity divided by the length can be thought of as a conductance that is equivalent to the heat or mass transfer coefficient. For each overall coefficient, there are two conductances: one associated with each half of the adjacent layers. Because conductances add as their inverse, it can be easily shown that $k_{\rm e,m}$, for example, is equal to the following

$$k_{\rm e,m} = \left(\frac{I_{\rm e}}{2D_{\rm e,t}} + \frac{I_{\rm m}}{2D_{\rm e,w}\lambda_{\rm e,m}}\right)^{-1}$$
 (A1)

Overall coefficients describing the diffusive transport for heat and mass from the midpoints of other compartments can be derived in a similar fashion.

Airway Lumen

Material balance. The molar balance of ethanol in the control volume of the airway can be written as

$$(\pi r^2 \Delta z) \frac{\partial (\mathbf{Y}_e \mathbf{N})}{\partial t} = (2\pi r \Delta z \delta) j_e + \dot{\mathbf{N}} \mathbf{Y}_e \big|_{z=z} - \dot{\mathbf{N}} \mathbf{Y}_e \big|_{z=z+\Delta z}$$
$$+ (\pi r^2 D_{e,a}) \left[\frac{\partial (\mathbf{Y}_e \mathbf{N})}{\partial z} \Big|_{z=z} - \frac{\partial (\mathbf{Y}_e \mathbf{N})}{\partial z} \Big|_{z=z+\Delta z} \right]$$
(A2)

where Y_e is the mole fraction of ethanol in air, N is the molar density of air, \dot{N} is the molar flow rate of air, j_e is the molar flux of ethanol from the mucous surface, δ is the ratio between the surface area of the control element of airway and a cylinder with the same volume, r is the radius of the airway, Δz is length of control element, and $D_{e,a}$ is the diffusivity of ethanol in air (cm²/s). By dividing Eq.~A2 by $\pi r^2 \Delta z$, taking the limit as $\Delta z \rightarrow 0$, and assuming that the molar concentration of gasses in the control volume with respect to time and position, and the molar flow rate of air traveling through the airways with respect to position, are constant, Eq.~A1 can be expanded and rearranged into

$$N\frac{\partial(Y_{e})}{\partial t} = \delta \frac{4j_{e}}{d} + \frac{4}{\pi d^{2}} \dot{N} \left(\frac{\partial Y_{e}}{\partial z} \right) + ND_{e,a} \left(\frac{\partial^{2} Y_{e}}{\partial z^{2}} \right)$$
(A3)

where d is diameter of the airway. The molar flux of ethanol between the airstream and the airway wall (mucous layer) can be described with the use of a local mass transfer coefficient k

$$j_{\rm e} = k_{\rm m,a}^{\rm e} (Y_{\rm e,wall} - Y_{\rm e}) \tag{A4}$$

where $Y_{e,\mathrm{wall}}$ is the mole fraction of ethanol in the gas phase at the lung wall in local equilibrium with the mole fraction of ethanol in the mucus.

Assuming that the air in the lungs behaves like an ideal gas, the governing equation can be obtained by combining $Eqs.\ A3$ and A4, and the ideal gas law

$$\frac{\partial (\mathbf{Y}_{e})}{\partial t} = \frac{4\delta P}{RT_{1}d} k_{m,a}^{e} (\mathbf{Y}_{e,wall} - \mathbf{Y}_{e}) + \frac{4\dot{\mathbf{V}}}{\pi d^{2}} \left(\frac{\partial \mathbf{Y}_{e}}{\partial z} \right) + D_{e,a} \left(\frac{\partial^{2} \mathbf{Y}_{e}}{\partial z^{2}} \right) \quad (A5)$$

where P is the total pressure, R is the ideal gas constant, T_l is the temperature of the air in the control volume, and \dot{V} is the volumetric flow rate.

Similar mass balance on water in the airway lumen results in the following governing equation for $Y_{\rm w}$

$$\frac{\partial (\mathbf{Y}_{\mathbf{w}})}{\partial t} = \frac{4\delta \mathbf{P}}{\mathbf{R}\mathbf{T}_{1}d} k_{\mathbf{m},\mathbf{a}}^{\mathbf{w}} (\mathbf{Y}_{\mathbf{w},\mathbf{wall}} - \mathbf{Y}_{\mathbf{w}}) + \frac{4\dot{\mathbf{V}}}{\pi d^{2}} \left(\frac{\partial \mathbf{Y}_{\mathbf{w}}}{\partial z} \right) + D_{\mathbf{e},\mathbf{a}} \left(\frac{\partial^{2} \mathbf{Y}_{\mathbf{w}}}{\partial z^{2}} \right) \tag{A6}$$

where $Y_{w,wall}$ is the mole fraction of water in the gas phase at the lung wall in local equilibrium with the mole fraction of water in the mucus, and $k_{a,m}^{w}$ is the local mass transfer coefficient for water between the airstream and the mucous layer.

Energy balance. The governing equation for the airway temperature is essentially the same as the one derived by Tsu et al. (36), except that the parameter δ was added into the model to describe the heat transfer from the mucous surface. The governing equation is shown below without derivation

Because it was assumed that the thickness of the mucous layer is very thin relative to the curvature of the airway, the control volume of the mucus can be approximated by $V_m = (\delta 2\pi r \Delta z) I_m$. V_m will change depending on the relative fluxes of fluids into the control volume. Assuming that all the fluids being transferred in and out of the mucus have the physical properties of water, the rate of the volume change can be expressed as

$$\frac{\partial (V_{\rm m})}{\partial t} = (\delta 2\pi r \Delta z) \frac{\partial (I_{\rm m})}{\partial t} = \frac{j_{\rm fluid}}{C} (\delta 2\pi r \Delta z) \tag{A10}$$

where j_{fluid} is the total molar flux of fluid into the mucous control volume (mol·s⁻¹·cm⁻²).

If the secretion rate of fluid from the epithelium to the mucus is equal to zero (when $I_{\rm m} > I_{\rm min}$), combining Eqs. A9

$$\frac{\partial (T_{l})}{\partial t} = \frac{4\dot{V}}{\pi d^{2}} \left(\frac{\partial T_{l}}{\partial z} \right) + \frac{\frac{4}{D} \frac{RT_{l}}{P}}{\hat{C}_{p,da}^{g} \frac{(273.15)}{(T_{a})} + \Delta \hat{C}_{p,e}^{g} Y_{e} + \Delta \hat{C}_{p,w}^{g} Y_{w}} * [(\hat{C}_{p,e}^{g} T_{m} - \Delta \hat{C}_{p,e}^{g} T_{a}) k_{m,a}^{e} (Y_{e,wall} - Y_{e}) + (\hat{C}_{p,w}^{g} T_{m} - \Delta \hat{C}_{p,w}^{g} T_{l}) k_{m,a}^{w} (Y_{w,wall} - Y_{w}) + h_{m,a} (T_{m} - T_{l})] \delta$$

$$(A7)$$

where $\hat{C}_{p,da}^g$ is the molar heat capacity of dry air, $\hat{C}_{p,w}^g$ is the molar heat capacity of water vapor, $\hat{C}_{p,e}^g$ is the molar heat capacity of ethanol vapor, $\Delta \hat{C}_{p,w}^g = \hat{C}_{p,w}^g - \hat{C}_{p,da}^g$, $\Delta \hat{C}_{p,e}^g = \hat{C}_{p,e}^g - \hat{C}_{p,da}^g$, and T_m is the average temperature of mucus in the control volume.

Mucus

Material balance. By assuming that the thickness of the mucous layer is thin relative to the curvature of the airway, the surface area at the epithelium-mucus interface is approximately equal to surface area at the mucus-air interface. This assumption, that the surface area on both sides of the mucous compartment is approximately equal, is also used for all the other compartments. As a result, the material balance for ethanol in the control volume can be written as

$$\begin{split} \frac{\partial (V_{m}X_{m}C)}{\partial t} &= \left[k_{e,m} \left(\frac{X_{e}C}{\lambda_{e,m}} - X_{m}C\right) \right. \\ &\left. - k_{m,a}^{e}(Y_{e,wall} - Y_{a}) + \frac{\dot{S}X_{e}}{\lambda_{e,m}}\right] (\delta 2\pi r \Delta z) \end{split} \label{eq:delta_e}$$

where $k_{e,m}$ is expressed in cm/s, V_m is the volume of mucous (ml), X_m is the average mole fraction of ethanol in mucous, X_e is the average mole fraction of ethanol in epithelium, $\lambda_{e,m}$ is the partition coefficient of ethanol between the mucous layer and the epithelium (equivalent to β_e/β_m), C is total molar concentration of the mucus (mol/ml), and S is secretion rate of fluid from the epithelium to mucus (mol·s⁻¹·cm⁻²).

If the molar concentration of the mucous layer is assumed to be constant, and equal to that of water, the previous equation can be expanded and rearranged into

$$\begin{split} \frac{\partial (\mathbf{X}_{\mathrm{m}})}{\partial t} &= \left(\frac{-\mathbf{X}_{\mathrm{m}}}{\mathbf{V}_{\mathrm{m}}} \right) \frac{\partial (\mathbf{V}_{\mathrm{m}})}{\partial t} + \left[k_{\mathrm{e,m}} \left(\frac{\mathbf{X}_{\mathrm{e}}}{\lambda_{\mathrm{e,m}}} - \mathbf{X}_{\mathrm{m}} \right) \right. \\ &\left. - k_{\mathrm{m,a}}^{\mathrm{e}} (\mathbf{Y}_{\mathrm{a,wall}} - \mathbf{Y}_{\mathrm{a}}) \frac{1}{\mathrm{C}} + \frac{\dot{\mathbf{S}}}{\mathrm{C}} \frac{\mathbf{X}_{\mathrm{e}}}{\lambda_{\mathrm{e,m}}} \right] \frac{(\delta 2 \pi r \Delta z)}{\mathrm{V}_{\mathrm{m}}} \end{split}$$

and A10 yields

$$\begin{split} \frac{\partial (\mathbf{X}_{\mathrm{m}})}{\partial t} &= \left(\frac{\mathbf{X}_{\mathrm{m}}}{I_{\mathrm{m}} \mathbf{C}} \right) j_{\mathrm{fluid}} \\ &+ \frac{1}{I_{\mathrm{m}}} \left[\mathbf{k}_{\mathrm{e,m}} \left(\frac{\mathbf{X}_{\mathrm{e}}}{\lambda_{\mathrm{e,m}}} - \mathbf{X}_{\mathrm{m}} \right) - k_{\mathrm{m,a}}^{\mathrm{e}} (\mathbf{Y}_{\mathrm{e,wall}} - \mathbf{Y}_{\mathrm{e}}) \frac{1}{\mathbf{C}} \right] \end{split} \tag{A11}$$

In this case, $j_{\rm fluid}$ is equal to the total molar flux at the air-mucus interface. The net molar flux of fluid at the mucus-epithelium interface is zero, since an equimolar counterdiffusion process occurs between water and ethanol. The total molar flux of fluid into the control element of mucus can then be expressed as

$$j_{\text{fluid}} = k_{\text{m,a}}^{\text{e}}(Y_{\text{e,wall}} - Y_{\text{e}}) + k_{\text{m,a}}^{\text{w}}(Y_{\text{w,wall}} - Y_{\text{w}})$$
 (A12)

Combining Eq. A11 with A12 yields

$$\begin{split} \frac{\partial (\mathbf{X}_{\mathrm{m}})}{\partial t} &= \frac{1}{I_{\mathrm{m}}} \left\{ k_{\mathrm{m,e}} \left(\frac{\mathbf{X}_{\mathrm{e}}}{\lambda_{\mathrm{e,m}}} - \mathbf{X}_{\mathrm{m}} \right) \right. \\ &\left. - \frac{(1 - \mathbf{X}_{\mathrm{m}})}{C} \left[k_{\mathrm{m,a}}^{\mathrm{e}} (\mathbf{Y}_{\mathrm{e,wall}} - \mathbf{Y}_{\mathrm{e}}) \right] \right. \\ &\left. + \left. \mathbf{X}_{\mathrm{m}} \left[k_{\mathrm{m,a}}^{\mathrm{w}} (\mathbf{Y}_{\mathrm{w,wall}} - \mathbf{Y}_{\mathrm{w}}) \right] \right\} \end{split}$$
(A13)

If the thickness of the mucous layer is equal to the minimum thickness, the mucus thickness is held constant, and fluid is secreted from the epithelium at the same rate at which it is being evaporated from the mucous surface. This process can be expressed as

$$\dot{S} = k_{ma}^{e} (Y_{e,wall} - Y_{e}) + k_{ma}^{w} (Y_{w,wall} - Y_{w})$$
 (A14)

and

$$\frac{\partial (\mathbf{V_m})}{\partial t} = \mathbf{0} \tag{A15}$$

Combining these two equations with Eq. A9 yields

$$\begin{split} \frac{\partial (\mathbf{X}_{m})}{\partial t} &= \frac{1}{I_{m}} \left| k_{e,m} \left(\frac{\mathbf{X}_{e}}{\lambda_{e,m}} - \mathbf{X}_{m} \right) - \frac{1}{C} \left[\left(1 - \frac{\mathbf{X}_{e}}{\lambda_{e,m}} \right) \right] \\ & \cdot \left[\mathbf{k}_{m,a}^{e} (\mathbf{Y}_{e,wall} - \mathbf{Y}_{e}) \right] + \frac{\mathbf{X}_{e}}{\lambda_{e,m}} \left[k_{m,a}^{w} (\mathbf{Y}_{w,wall} - \mathbf{Y}_{w}) \right] \end{split}$$
(A16)

Thus the governing equation for X_m can be expressed by Eq. A13 if \dot{S} is equal to zero or by Eq. A16 if \dot{S} is nonzero.

Energy balance. The energy balance is performed in a manner similar to the mass balance; the resulting governing equation for T_m is shown below without detailed derivation

the control element of tissue bed, $V_{c,t}$ is the volume that capillaries occupy in the tissue control element, and V_t is the volume that tissue mass occupies in the control element.

The fluid that is secreted to the epithelium is replaced by fluids filtered in by the capillaries. The volume of the tissue mass is assumed to be constant; therefore, the secretion and filtration process must occur at the same rate.

Material balance. The ratio between the volume of the capillaries and the total volume of the tissue $(\varphi_{c,t})$ can be expressed as

$$\phi_{c,t} = \frac{V_{c,t}}{V_{T,t}} \tag{A20}$$

$$\begin{split} \frac{\partial T_{m}}{\partial t} &= \frac{-T_{m}}{I_{m}} \left(\frac{\partial I_{m}}{\partial t} \right) + \frac{1}{C\hat{C}_{p,w}^{1} I_{m}} \left[h_{e,m} (T_{e} - T_{m}) - h_{m,a} (T_{m} - T_{l}) + \dot{S}\hat{C}_{p,w}^{l} (T_{e} - T_{m}) \right] \\ &+ \frac{1}{C\hat{C}_{p,w}^{l} I_{m}} \left[\left[\Delta H_{v,w} + T(\hat{C}_{p,w}^{g} - \hat{C}_{p,w}^{l}) \right] k_{m,a}^{w} (Y_{w,wall} - Y_{w}) + \left[\Delta H_{v,e} + T(\hat{C}_{p,e}^{g} - \hat{C}_{p,e}^{l}) \right] k_{m,a}^{e} (Y_{e,wall} - Y_{e}) \right] \end{split}$$

where $\Delta H_{v,w}$ and $\Delta H_{v,e}$ are the latent of heats of vaporization of water and ethanol, respectively.

Epithelium

Material balance. By assuming that the molar concentration of fluids and the volume of epithelium tissue are constant in the control element, the governing equation for the epithelium can be written as

$$\begin{split} &\frac{\partial (\mathbf{X_e})}{\partial t} \\ &= \frac{1}{I_e} \left[k_{t,e} \left(\frac{\mathbf{X_t}}{\lambda_{t,e}} - \mathbf{X_e} \right) - k_{e,m} \left(\frac{\mathbf{X_e}}{\lambda_{e,m}} - \mathbf{X_m} \right) + \frac{\dot{\mathbf{S}}}{\mathbf{C}} \left(\frac{\mathbf{X_t}}{\lambda_{t,e}} - \mathbf{X_e} \right) \right] \end{split} \tag{A18}$$

where $\emph{k}_{t,e}$ is the overall mass transfer coefficient between the tissue layer and the epithelium (cm/s), and \emph{X}_t is the average mole fraction of ethanol in the tissue.

Energy balance. Using the same assumptions for the energy balance, the governing equation can be written as

$$\frac{\partial (T_{e})}{\partial t} = \frac{[h_{t,e}(T_{t} - T_{e}) - h_{e,m}(T_{e} - T_{m})]}{I_{e}\hat{C}_{n,e}C} + \frac{\dot{S}}{C} \frac{(T_{t} - T_{e})}{I_{e}} \quad (A19)$$

The total volume of the tissue bed may be expressed in terms of the dimension of the control element as $V_{T,t} = (A_d) \, \mathit{l}_t$, which, when combined with previous definitions of $V_{T,t}$ and $\mathit{Eq. A20}$, produces the following expression for V_t

$$V_{t} = I_{t}A_{d} \left(1 - \phi_{c,t}\right) \tag{A21}$$

The material balance on the tissue mass can then be written as

$$\frac{\partial (\mathbf{V}_{t} \mathbf{X}_{t})}{\partial t} = k_{s,t} \left(\frac{\mathbf{X}_{s}}{\lambda_{s,t}} - \mathbf{X}_{t} \right) (A_{d}) - k_{t,e} \left(\frac{\mathbf{X}_{t}}{\lambda_{t,e}} - \mathbf{X}_{e} \right) (A_{d}) \\
+ \frac{D_{e,w}}{r_{c}} \left(\frac{\mathbf{X}_{c,t}}{\lambda_{c,t}} - \mathbf{X}_{t} \right) A_{c,t} + \frac{\dot{\mathbf{S}}}{\mathbf{C}} \left(\frac{\mathbf{X}_{c,t}}{\lambda_{c,t}} - \mathbf{X}_{t} \right) (A_{d}) \tag{A22}$$

where $A_{c,t}$ is the surface area between the capillaries and the tissue mass (defined below), $\lambda_{s,t}$ is the smooth muscle-tissue partition coefficient, $k_{s,t}$ is the capillary-tissue partition coefficient, $k_{s,t}$ is the overall mass transfer coefficient between the smooth muscle and the tissue layer (cm/s), $D_{e,w}$ is the diffusivity of ethanol in water (cm²/s), and X_s is the average mole fraction of ethanol in the smooth muscle layer. The governing equation is obtained by expanding the derivative and inserting Eq.~A21 to get

$$\frac{\partial (\mathbf{X}_{t})}{\partial t} = \frac{k_{s,t} \left(\frac{\mathbf{X}_{s}}{\lambda_{s,t}} - \mathbf{X}_{t} \right) - k_{t,e} \left(\frac{\mathbf{X}_{t}}{\lambda_{t,e}} - \mathbf{X}_{e} \right) + \frac{\dot{\mathbf{S}}}{\mathbf{C}} \left(\frac{\mathbf{X}_{c,t}}{\lambda_{c,t}} - \mathbf{X}_{t} \right) + \frac{D_{e,w}}{r_{c}} \left(\frac{\mathbf{X}_{c,t}}{\lambda_{c,t}} - \mathbf{X}_{t} \right) \xi_{c,t}}{I_{t} (1 - \phi_{c,t})}$$
(A23)

where $h_{t,e}$ is the overall heat transfer coefficient between the connective tissue and epithelium, and T_t is the average temperature of the tissue layer (K).

Connective Tissue

Each control volume of tissue is assumed to have a network of capillaries, which supplies blood at the condition of the body and exits at a new condition that is determined by the dynamics of heat and mass transfer. The total volume of the perfused tissue is assumed to be made up of tissue and capillaries: $V_{T,t} = V_{c,t} + V_t$, where $V_{T,t}$ is the total volume of

where $\xi_{c,t} = A_{c,t}/A_d$. $\xi_{c,t}$ can be calculated from the thickness of the tissue bed, the volume fraction of capillaries, and the average radius of each capillary. The total surface area of the capillaries is equal to the number of capillaries (n_c) times the surface area of each capillary, $A_{c,t} = n_c(2\pi r_c \Delta z)$. The number of capillaries can be determined by Eq.~4; thus $\xi_{c,t}$ can be expressed as

$$\xi_{c,t} = \frac{A_{c,t}}{A_d} = \frac{2I_t \phi_{c,t}}{r_c} \tag{A24}$$

Energy balance. In an analogous fashion, the governing equation for the temperature of the tissue mass can be derived as

perfused tissue bed, except there are no secretion or filtration terms in the equations. The governing equations for the mole fraction of ethanol and the temperature of the smooth muscle

$$\frac{\partial (T_{t})}{\partial t} = \frac{h_{s,t}(T_{s} - T_{t}) - h_{t,e}(T_{t} - T_{e}) + \frac{\kappa_{w}}{r_{c}}(T_{c,t} - T_{t})\xi_{1} + \dot{S}\hat{C}_{p,t}(T_{c,t} - T_{t})}{(1 - \phi_{c,t})I_{t}\hat{C}_{p,t}C}$$
(A25)

where $h_{s,t}$ is the overall heat transfer coefficient between the connective tissue and smooth muscle, T_s is the average temperature of the smooth muscle layer, and κ_w is the thermal conductivity of water.

Capillary Bed of Connective Tissue

Material balance. The tissue layer is assumed to be perfused by a bed of capillaries, which is distributed uniformly within the tissue mass. The blood that enters the control volume is assumed to be in equilibrium with the body [i.e., 37° C and the blood ethanol mole fraction (X_a)]. The temperature and ethanol concentration of the blood exiting the control volume is determined by the heat and mass transfer dynamics. The material balance on the capillaries can be written as

$$\begin{split} \frac{\partial (V_{c,t}CX_{c,t})}{\partial t} &= \dot{q}_{br,t}CX_{a} - (\dot{q}_{br,t} - \dot{S})X_{c,t}C - \dot{S}X_{c,t}C \\ &- \frac{D_{e,w}}{r_{c}} C \left(\frac{X_{c,t}}{\lambda_{c,t}} - X_{t} \right) A_{c,t} \end{split} \tag{A26}$$

where $X_{\rm c,t}$ is the average mole fraction of ethanol in the tissue capillary. The flux of ethanol into the tissue from the capillaries is described by the fourth term on the right-hand side of Eq.~A26. This was derived by assuming that the average concentration of ethanol is at the center of the capillary and that there exists a linear concentration gradient from the center of the capillary to the capillary wall. Assuming that the total molar concentration and volume of the capillaries are constant, and substituting the relationships for V_c and $A_{c,t}$. Eq.~A26 can be written in the final form as

$$\frac{\partial (X_{c,t})}{\partial \textit{t}} = \frac{1}{\tau_t} \left(X_a - X_{c,t} \right) - \frac{D_{e,w}}{\textit{r}_c \varphi_{c,t} \textit{I}_t C} \left(\frac{X_{c,t}}{\lambda_{c,t}} - X_t \right) \xi_{t,c} \quad \textit{(A27)}$$

where τ_t is the mean residence time $(V_{c,t}/\dot{q}_{br,t})$ of blood in the tissue capillary.

Energy balance. The governing equation for the temperature of the capillary bed can be derived by a similar fashion and is shown below without derivation

$$\frac{\partial (T_{c,t})}{\partial t} = \frac{1}{\tau_t} (T_{body} - T_{c,t}) - \frac{\kappa_w}{r_c \varphi_{c,t} I_t \hat{C}_{n,b} C} (T_{c,t} - T_t) \xi_{c,t} \quad (A28)$$

Smooth Muscle

The smooth muscle lies between a body layer and a perfused tissue layer. The smooth muscle is also perfused by a network of capillaries. The derivations of the governing equations for the smooth muscle are similar to these of the

are presented below without detailed derivation

$$\frac{\partial (\mathbf{X_s})}{\partial t}$$

$$= \frac{k_{\text{b,s}} \left(\frac{\mathbf{X}_{\text{b}}}{\lambda_{\text{b,s}}} - \mathbf{X}_{\text{s}}\right) - k_{\text{s,t}} \left(\frac{\mathbf{X}_{\text{s}}}{\lambda_{\text{S,t}}} - \mathbf{X}_{\text{t}}\right) + \frac{D_{\text{e,w}}}{r_{\text{c}}} \left(\frac{\mathbf{X}_{\text{c,s}}}{\lambda_{\text{b,t}}} - \mathbf{X}_{\text{s}}\right) \xi_{\text{c,s}}}{I_{\text{s}} (1 - \phi_{\text{c,s}})} \quad (A29)$$

where $\varphi_{c,s}$ is the ratio between the volume of the capillaries and the volume of smooth muscle and

$$\frac{\partial (T_{s})}{\partial t} = \frac{h_{b,s}(T_{b} - T_{s}) - h_{s,t}(T_{s} - T_{t}) + \frac{\kappa_{w}}{r_{c}}(T_{c,s} - T_{s}) \, \xi_{c,s}}{(1 - \phi_{c,s})\hat{C}_{p,s} \, I_{s}C} \tag{A30}$$

where X_b is the average mole fraction of ethanol in the body layer, $k_{b,s}$ is the overall mass transfer coefficient between the smooth muscle and the body layer, $h_{b,s}$ is the overall heat transfer coefficient between the body layer and the smooth muscle, T_b is the average temperature of the body layer, and $\xi_{c,s}$ and $\varphi_{c,s}$ describe the surface area of the smooth muscle layer in a fashion analogous to $\xi_{c,t}$ and $\varphi_{c,t}$.

Capillary Bed of Smooth Muscle

Although the capillaries in the smooth muscle do not secrete fluids into the smooth muscle mass, the governing equations for the capillaries have the same form as the tissue layer and are shown below without detailed derivation

$$\frac{\partial (\mathbf{X}_{\text{c,s}})}{\partial t} = \frac{1}{\tau_{\text{s}}} \left(\mathbf{X}_{\text{body}} - \mathbf{X}_{\text{c,s}} \right) - \frac{D_{\text{e,w}}}{r_{\text{c}} \phi_{\text{c,s}} I_{\text{s}} C} \left(\frac{\mathbf{X}_{\text{c,s}}}{\lambda_{\text{c,t}}} - \mathbf{X}_{\text{t}} \right) \xi_{\text{c,s}} \quad (A31)$$

and

$$\frac{\partial (T_{c,s})}{\partial \it{t}} = \frac{1}{\tau_s} \left(T_{body} - T_{c,s} \right) - \frac{\kappa_w}{\it{r}_c \varphi_{c,s} \it{I}_s \hat{C}_{p,s} C} \left(T_{body} - T_t \right) \, \xi_{c,s} \quad (\it{A32}$$

where τ_s is the mean residence time $(V_{e,s}/\dot{q}_{br,s})$ of blood in the tissue capillary.

Body-Tissue Layer

Similar to the previous equations, the governing equations for the body layer are obtained by performing a material and energy balance. The governing equations for the body layer are shown below without detailed derivation

$$\frac{\partial (X_b)}{\partial t} = \frac{k_{b,b}(X_{body} - X_b) - k_{b,s} \left(\frac{X_b}{\lambda_{b,s}} - X_s\right)}{I_b}$$
(A33)

and

$$\frac{\partial (T_b)}{\partial t} = \frac{h_{b,b}(T_{body} - T_b) - h_{b,s}(T_b - T_s)}{I_b \gamma \hat{C}_{p,w}^l C}$$
(A34)

where $k_{b,b}$ is the overall mass transfer coefficient between the body and the body layer, and $h_{b,b}$ is the overall heat transfer coefficient between the body layer and the body.

This work was supported by generous start-up funds to S. C. George from the Department of Chemical and Biochemical Engineering and Materials Science at the University of California, Irvine.

Address for reprint requests: S. C. George, Dept. of Chemical and Biochemical Engineering and Materials Science, 916 Engineering Tower, Univ. of California, Irvine, CA 92697-2575.

Received 3 April 1997; accepted in final form 9 February 1998.

REFERENCES

- Aharonson, E. F., H. Menkes, G. Gurtner, D. L. Swift, and D. F. Proctor. Effect of respiratory airflow rate on the removal of soluble vapors by the nose. *J. Appl. Physiol.* 37: 654–657, 1974.
- Bernard, S. L., R. W. Glenny, N. Polisar, D. L. Luchtel, and S. Lakshminarayan. Distribution of pulmonary and bronchial blood supply to airways measured by fluorescent microspheres. J. Appl. Physiol. 80: 430–436, 1996.
- 3. Bird, R. B., W. E. Stewart, and E. N. Lightfoot. Transport Phenomena. New York: Wiley, 1960, p. 406.
- Cander, L., and R. E. Forster. Determination of pulmonary parenchymal tissue volume and pulmonary capillary blood flow in man. J. Appl. Physiol. 14: 541–551, 1959.
- Chilton, T. H., and A. P. Colburn. Mass transfer (absorption) coefficients: prediction from data on heat transfer and fluid friction. *Ind. Eng. Chem.* 26: 1183–1187, 1934.
- Dahl, A. R., M. B. Snipes, and P. Gerde. Sites for uptake of inhaled vapors in beagle dogs. *Toxicol. Appl. Pharmacol.* 109: 263–275, 1991.
- Derwent, R., and O. Hov. Application of sensitivity and uncertainty analysis techniques to a photochemical ozone model. *J. Geophys. Res.* 93: 5185–5199, 1988.
- Dubois, A. B., and R. M. Rogers. Respiratory factors determining the tissue concentrations of inhaled substances. *Respir. Physiol.* 5: 34–52, 1968.
- 9. **Eroschenko, V. P.** Atlas of Histology With Functional Correlations. Baltimore, MD: Williams & Wilkins, 1996, p. 227.
- Gastineau, R. M., P. J. Walsh, and N. Underwood. Thickness of the bronchial epithelium with relation to exposure to radon. *Health Phys.* 23: 857–860, 1972.
- George, S. C., A. L. Babb, M. E. Deffebach, and M. P. Hlastala. Diffusion of nonelectrolytes in the canine trachea: effect of tight junction. *J. Appl. Physiol.* 80: 1687–1695, 1996.
- George, S. C., A. L. Babb, and M. P. Hlastala. Dynamics of soluble gas exchange in the airways. III. Single exhalation breathing maneuver. J. Appl. Physiol. 75: 2439–2449, 1993.
- George, S. C., A. L. Babb, and M. P. Hlastala. Modeling the concentration of ethanol in the exhaled breath following pretest breathing maneuvers. *Ann. Biomed. Eng.* 23: 48–60, 1995.
- George, S. C., J. E. Souders, A. L. Babb, and M. P. Hlastala. Modeling steady state inert-gas exchange in the canine trachea. *J. Appl. Physiol.* 79: 929–940, 1995.
- 15. **Hanna, L. M.** *Modeling of Heat and Water Vapor Transport in the Human Respiratory Tract* (PhD thesis). Philadelphia, PA: Univ. of Pennsylvania, 1983.
- Hildebrandt, J. Structural and mechanical aspects of respiration. In: *Textbook of Physiology*, edited by H. D. Patton, A. F. Fuchs, B. Hille, A. M. Scher, and R. Steiner. Philadelphia, PA: Saunders, 1989, vol. 2, p. 995.
- Hindmarsh, A. LSODE (computer software). Lawrence Livermore Laboratory, Livermore, CA, 1981.
- Ingenito, E. P. Respiratory Fluid Mechanics and Heat Transfer (PhD thesis). Cambridge, MA: Massachusetts Institute of Technology, 1984.

- James, A. L., P. D. Paré, and J. C. Hogg. Effects of lung volume, bronchoconstriction, and cigarette smoke on morphometric airway dimensions. *J. Appl. Physiol.* 64: 913–919, 1988.
- 20. **Jones, A. W.** Quantitative measurements of the alcohol concentration and the temperature of breath during a prolonged exhalation. *Acta Physiol. Scand.* 114: 407–412, 1982.
- Jones, A. W. Determination of liquid/air partition coefficients for dilute solutions of ethanol in water, whole blood, and plasma. *J. Anal. Toxicol.* 7: 193–197, 1983.
- Laitinen, A., L. A. Laitinen, R. Moss, and J. G. Widdicombe.
 Organisation and structure of the tracheal and bronchial blood
 vessels in the dog. J. Anat. 165: 133–140, 1989.
- 23. **Laitinen, L. A., and A. Laitinen.** The bronchial circulation: histology and electron microscopy. In: *The Bronchial Circulation*, edited by J. Butler. New York: Dekker, 1992, vol. 57, p. 79–106. (Lung Biol. Health Dis. Ser.)
- 24. Lopez-Vidriero, M. T., I. Das, and L. M. Reid. Airway secretion: source, biochemical and rheological properties. In: *Respiratory Defense Mechanisms*, edited by J. D. Brain, D. F. Proctor, and L. M. Reid. New York: Dekker, 1977, vol. 5, pt. 1, p. 289–356. (Lung Biol. Health Dis. Ser.)
- Luchtel, D. L. The mucous layer of the trachea and major bronchi in the rat. Scand. Electr. Micro. 2: 1089–1098, 1978.
- Matsuba, K., and W. M. Thurlbeck. A morphometric study of bronchial and bronchiolar walls in children. *Am. Rev. Respir. Dis.* 105: 908–913, 1972.
- 27. McKay, M. D., R. J. Beckman, and W. J. Conover. A comparison of three methods for selecting values of input variables in the analysis of output from a computer code. *Technometrics* 21: 239–245, 1979.
- Newman, W. H., and P. P. Lele. A transient heating technique for the measurement of thermal properties of perfused biological tissue. *J. Biomech. Eng.* 107: 219–227, 1985.
- Scherer, P. W., L. H. Shendalman, N. M. Greene, and A. Bouhuys. Measurement of axial diffusivities in a model on the bronchial airways. *J. Appl. Physiol.* 38: 719–723, 1975.
- Schrikker, A. C. M., W. R. de Vries, A. Zwart, and S. C. M. Luijendijk. Uptake of highly soluble gases in the epithelium of the conducting airways. *Pflügers Arch.* 405: 389–394, 1985.
- Schrikker, A. C. M., W. R. de Vries, A. Zwart, and S. C. M. Luijendijk. The excretion of highly soluble gases by the lung in man. *Pflügers Arch*. 415: 214–219, 1989.
- Sleigh, M. A., J. R. Blake, and N. Liron. The propulsion of mucus by cilia. Am. Rev. Respir. Dis. 137: 726-741, 1988.
- 33. Solway, J., A. R. Leff, İ. Dreshaj, N. M. Munoz, E. P. Ingenito, D. Michaels, R. H. Ingram, and J. M. Drazen. Circulatory heat sources for canine respiratory heat exchange. *J. Clin. Invest.* 78: 1015–1019, 1986.
- Solway, J., B. H. Pichurko, E. P. Ingenito, E. R. McFadden, Jr., C. H. Fanta, R. H. Ingram, Jr., and J. M. Drazen. Breathing pattern affects airway wall temperature during cold air hyperpnea in humans. Am. Rev. Respir. Dis. 132: 853–857, 1985
- Souders, J. E., S. C. George, N. L. Polissar, E. R. Swenson, and M. P. Hlastala. Tracheal gas exchange: perfusion-related differences in inert-gas elimination. *J. Appl. Physiol.* 79: 918– 928, 1995.
- 36. Tsu, M. E., A. L. Babb, E. M. Sugiyama, and M. P. Hlastala. Dynamics of soluble gas exchange in the airways. II. Effects of breathing conditions. *Respir. Physiol.* 83: 261–276, 1991.
- Tsu, M. E., A. L. Babb, D. D. Ralph, and M. P. Hlastala. Dynamics of heat, water, and soluble gas exchange in the human airways. I. A model study. *Ann. Biomed. Eng.* 16: 547–571, 1988.
- Wagner, E. M., and W. A. Mitzner. Contribution of pulmonary vs. systemic perfusion of airway smooth muscle. *J. Appl. Physiol.* 78: 403–409, 1995.
- Weibel, E. Morphometry of the Human Lung. New York: Springer-Verlag, 1963, p. 139.
- Wiedeman, M. P. Architecture. In: Handbook of Physiology. The Cardiovascular System. Microcirculation. Bethesda, MD: Am. Physiol. Soc., 1987, vol. 4, sect. 2, pt. 1, chapt. 2, p. 11–40.